Electrodynamics of superconductor-ferromagnet hybrid structures

A.S.Mel'nikov

Institute for Physics of Microstructures RAS

IPM RAS

S.V.Mironov
A.V.Samokhvalov
D.Vodolazov
Yu.Erin
A.Bespalov

V.Vadimov
M.Sapozhnikov

Universite Bordeaux I, France

A.I.Buzdin

Outline

- **Interplay of magnetism and superconductivity and elecrodynamic phenomena**
- **Orbital effect of stray magnetic fields on superconductivity nucleation and inhomogeneous states**
- **Effect of superconductivity on the domain structure**
- **Proximity effect and its influence on the electrodynamic response**
- **Spontaneous currents**
- **LOFF instabilities**

Mechanisms of interaction of superconducting and magnetic order parameters

Stray magnetic field affects the electron trajectories

Exchange field affects spin orientation

V.L.Ginzburg (1956)

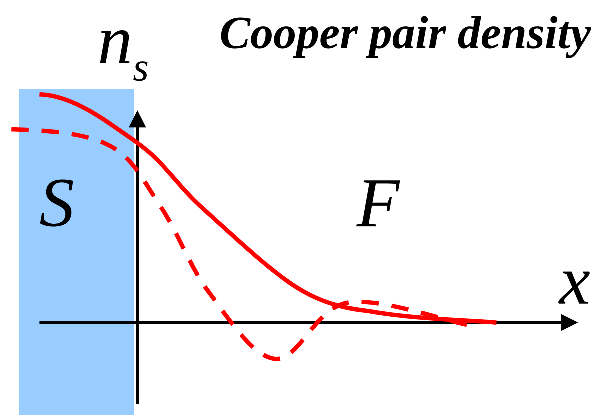

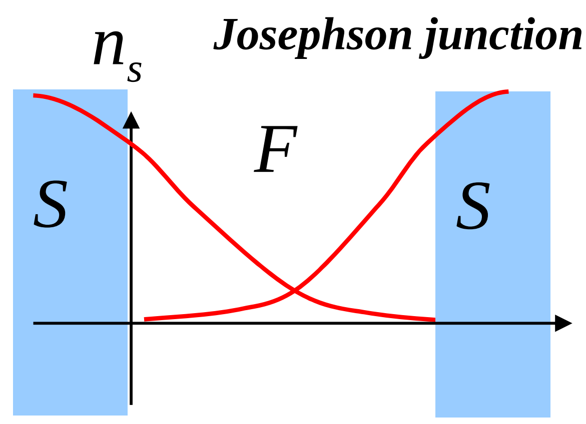

Something is forgotten?

1. ***Interference effects (oscillations of the Cooper pair wavefunction)***

2. ***Generation of triplet Cooper pairs***

Structures and materials

Ferromagnetic superconductors

UGe_2 , URhGe

ErRh4B4, ErNi2B2C

$EuFe_2(As_{1-x}P_x)_2$

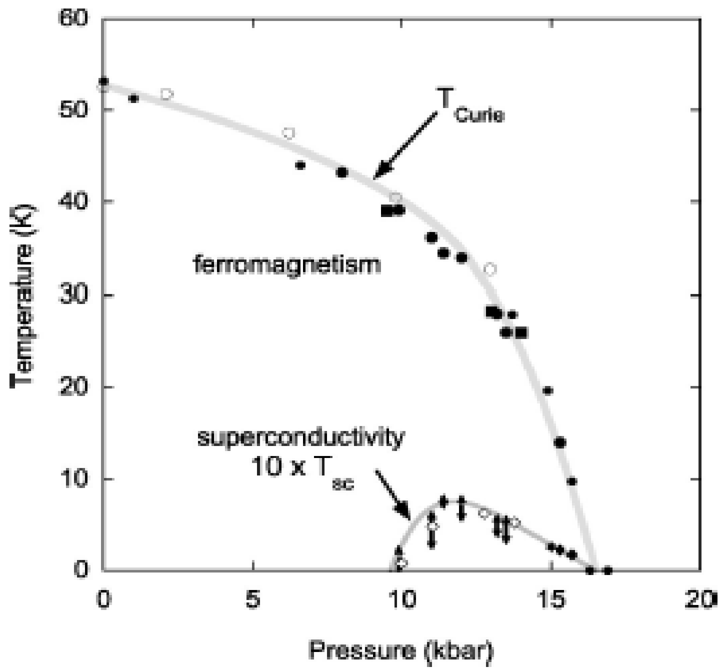

Superconductor-ferromagnet hybrid structures

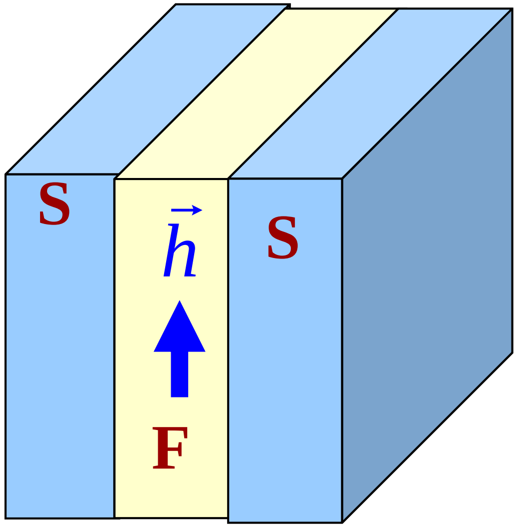

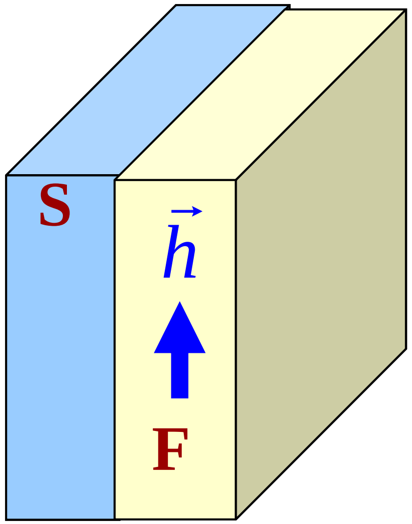

Ginzburg-Landau theory

$$-\frac{\hbar^2}{4m}\left(\nabla-\frac{2ie}{\hbar c}\vec{A}\right)^2\Psi+a\Psi+b|\Psi|^2\Psi=0$$

$$rot\vec{B}=\frac{4\pi}{c}\vec{j}$$

$$\vec{j}=-\frac{ie\hbar}{2m}\left(\Psi^*\nabla\Psi-\Psi\nabla\Psi^*\right)-\frac{2e^2}{mc}|\Psi|^2\vec{A}$$

$$\vec{j}=\frac{e\hbar}{m}|\Psi|^2\left(-\frac{2e}{\hbar c}\vec{A}+\nabla\varphi\right)$$

$$\vec{j}=-\frac{e^2n_s}{mc}\vec{A}$$

London equation

Boundary conditions

I-S

$$\vec{n}\left(\nabla\Psi-\frac{2ie}{\hbar c}\vec{A}\Psi\right)=0$$

N-S

$$\Psi=0$$

Localized superconducting channels.
Domain wall superconductivity

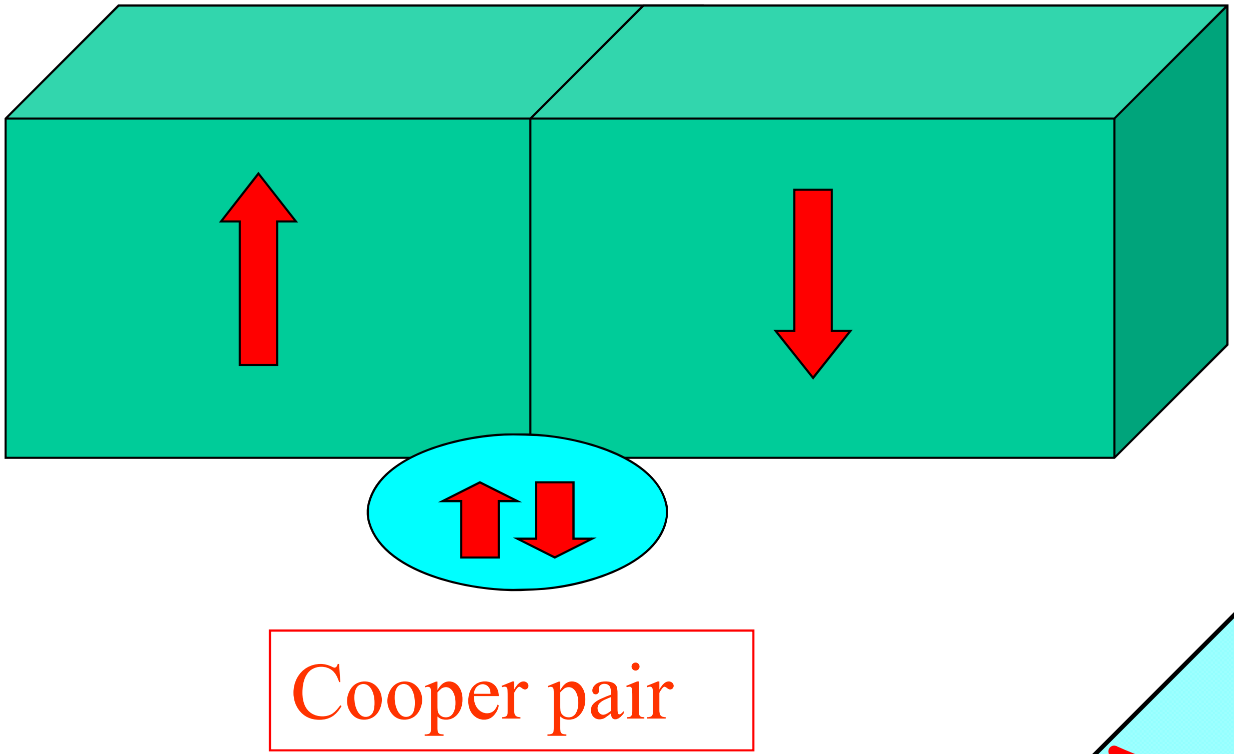

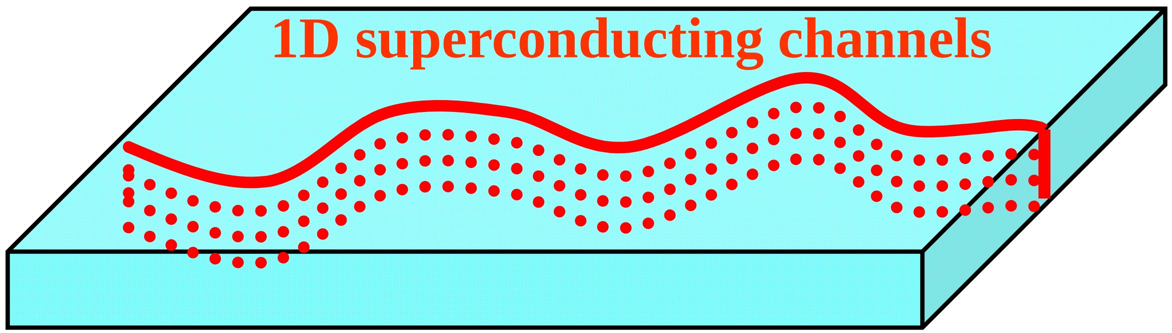

Electromagnetic (orbital) mechanism. Phenomenological Ginzburg-Landau theory

External field H **+** **Inhomogeneous magnetic field induced by magnetic moments**

$$-\left(\nabla + \frac{2\pi i}{\Phi_0}\vec{A}(\vec{r})\right)^2 \Psi = \frac{1}{\xi^2(T)}\Psi$$

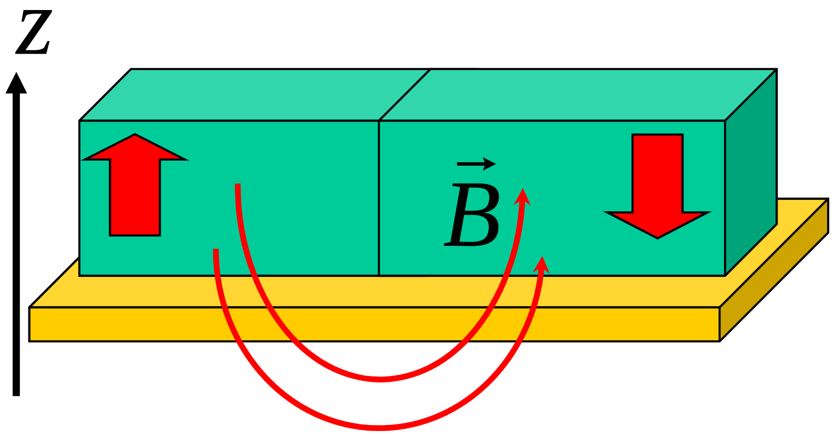

$$H_{c2}^{\perp} << H_{c2}^{\parallel}$$

Thin superconducting films: Only B_z field component is important

Assumption: Domain walls are pinned

Superconductivity nucleation in S/F bilayers

Narrow domains

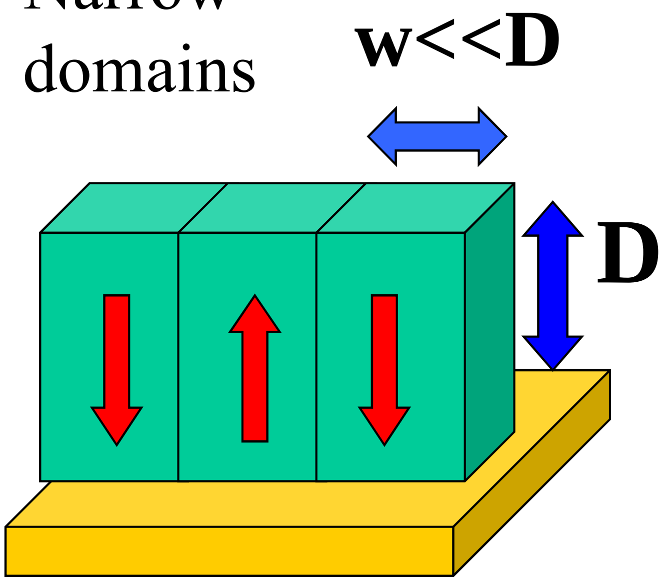

T_c of a nucleus localized at a single domain wall

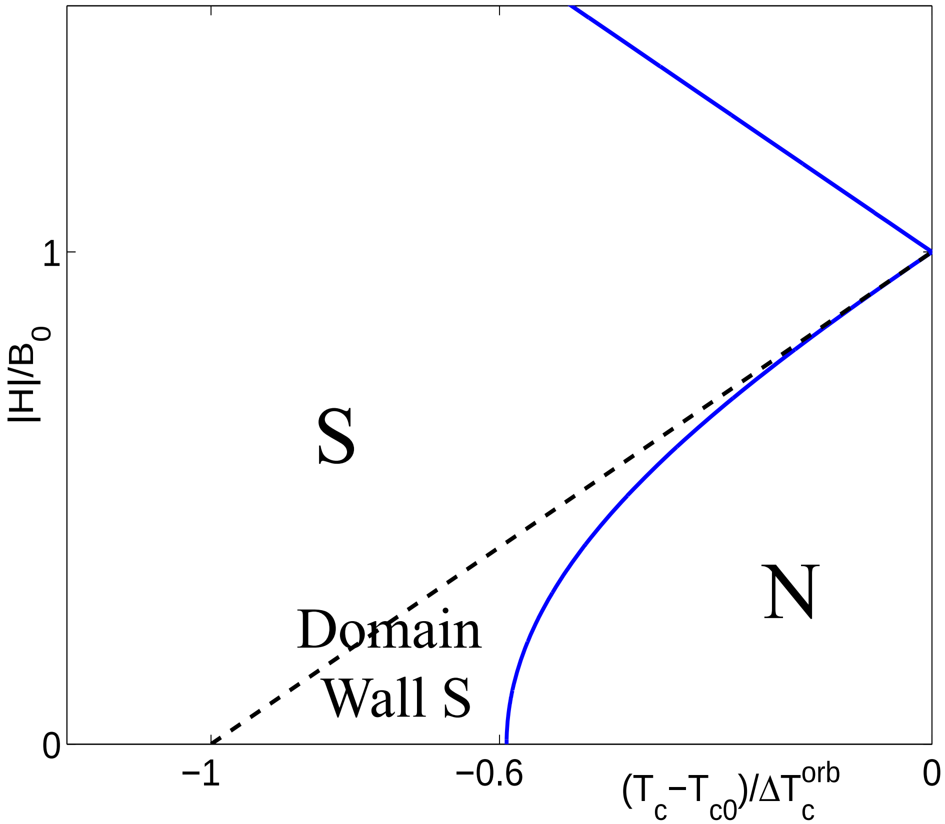

Nb/F

$$4\pi M \sim 1-10\,kOe \qquad \frac{dH_{c2}}{dT} \sim 0.5\,kOe\,/\,K$$

$$T_c \sim 9\,K \qquad \delta T_c \sim 1-3\,K$$

Superconducting nucleus in a periodic domain structure in an external field

$$H \neq 0$$

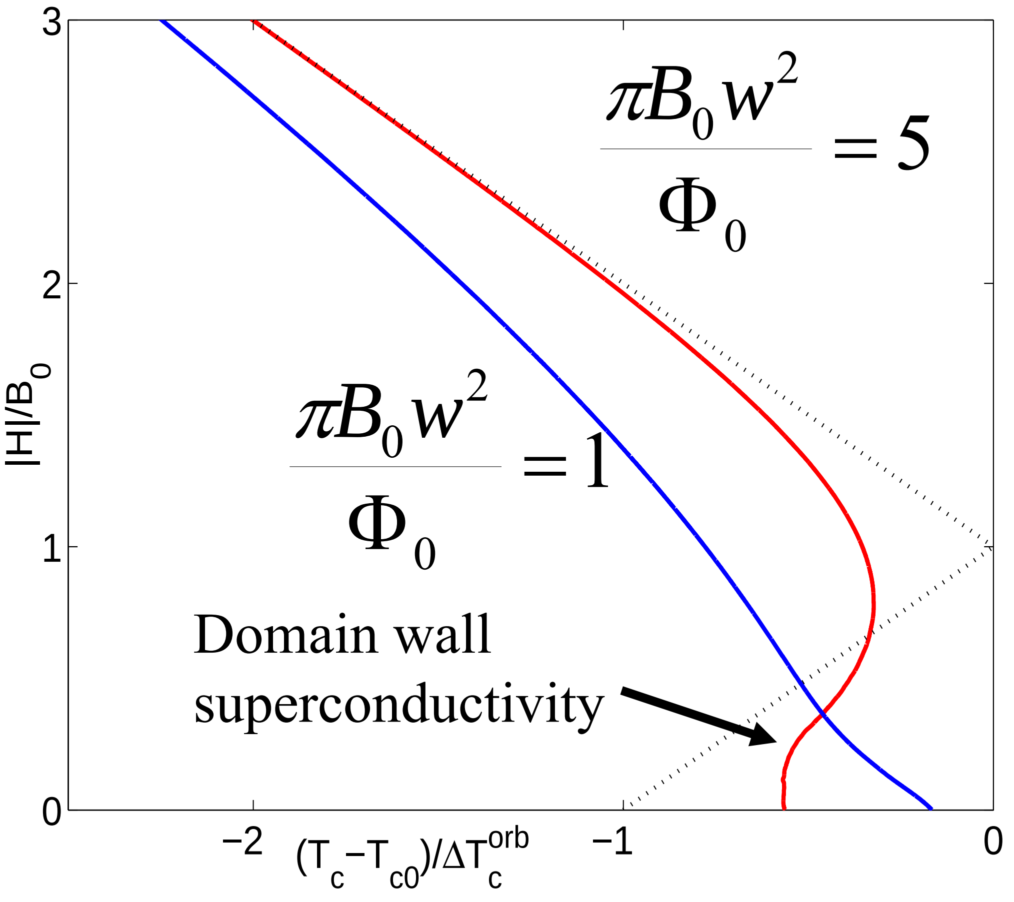

$$\frac{B_0 w^2}{\Phi_0} >> 1$$

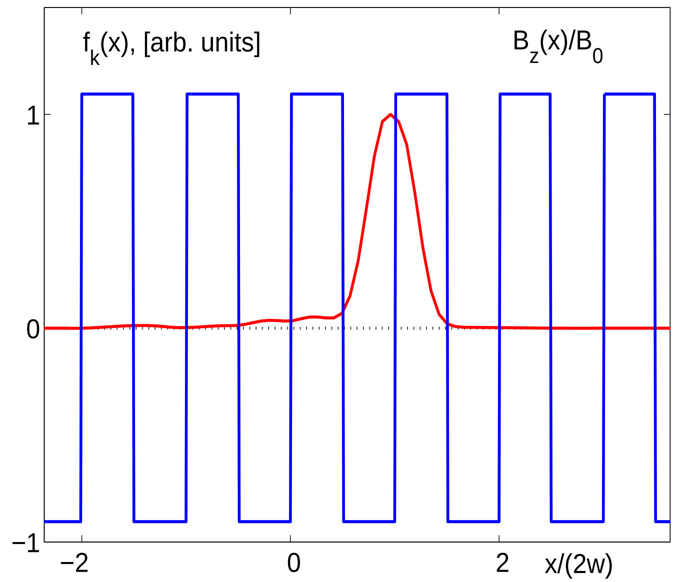

$$\frac{B_0 w^2}{\Phi_0} << 1$$

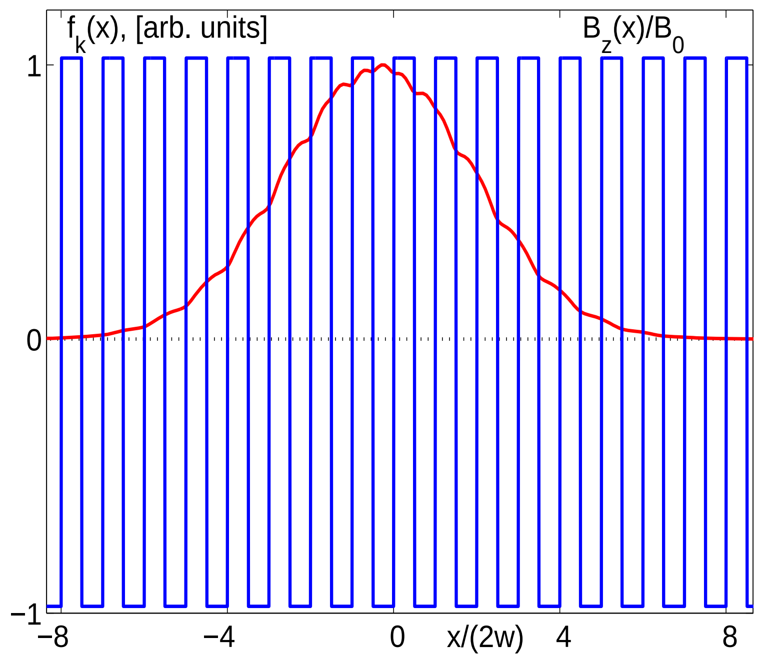

Upper critical field in the presence of domain structure

Phys.Rev.Lett (2005), Phys.Rev.B (2007-2008)

CoPt / Nb / CoPt:

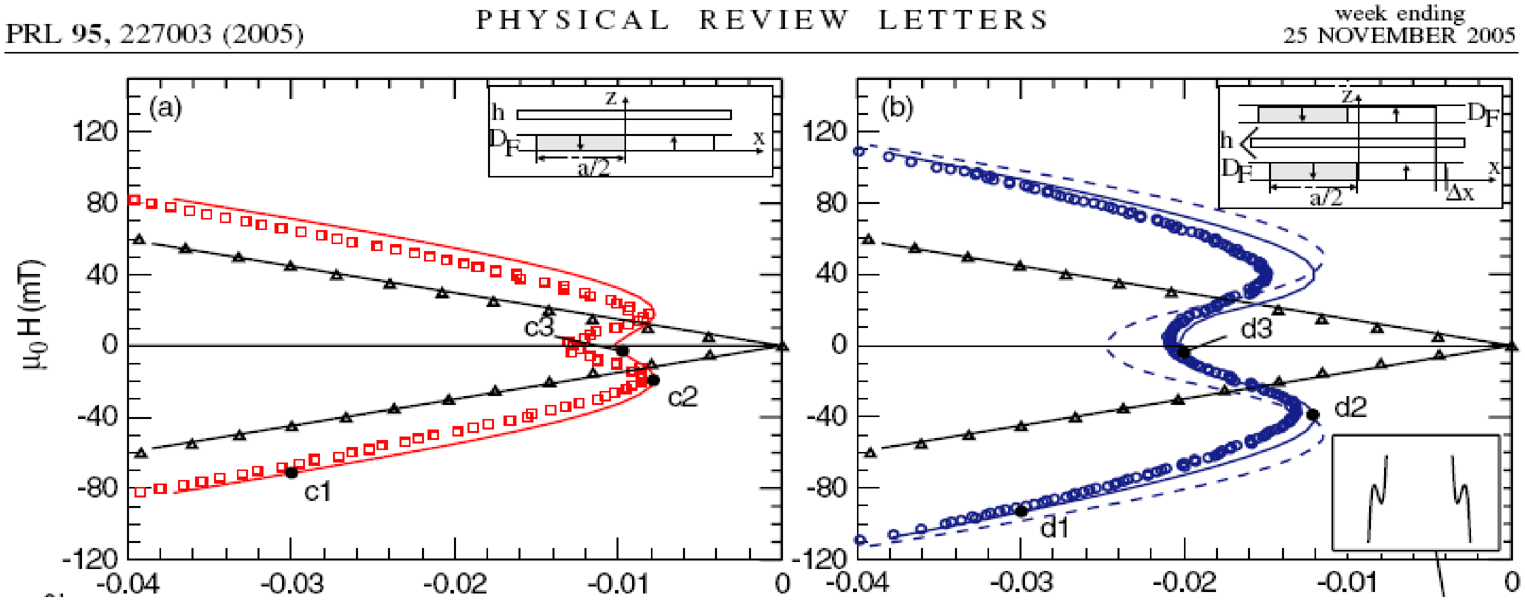

CoPt / Al:

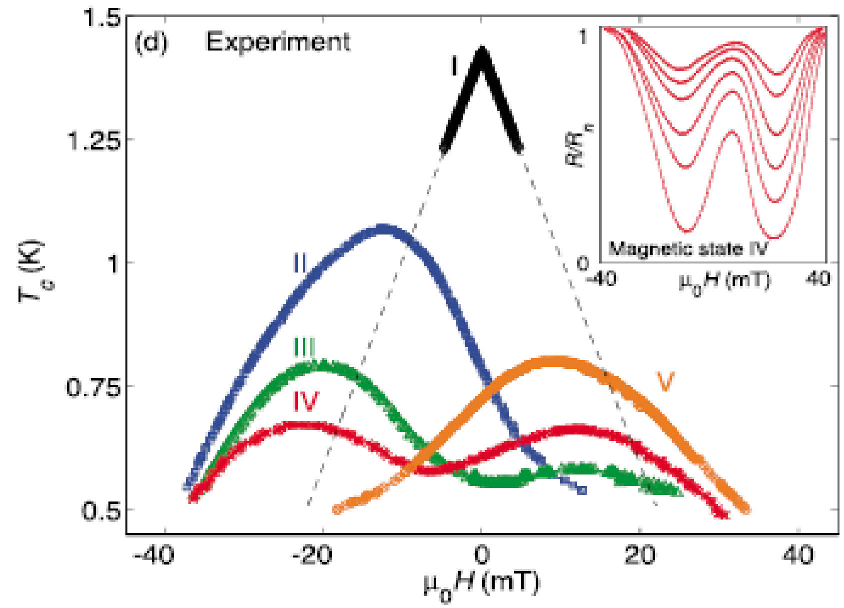

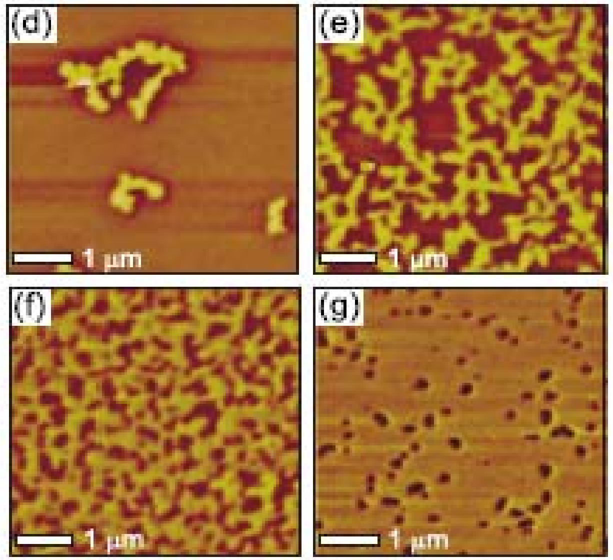

Domain superconductivity measured by scanning laser microscopy

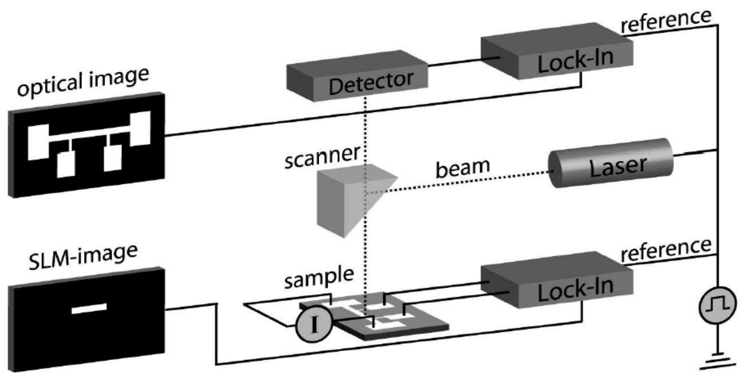

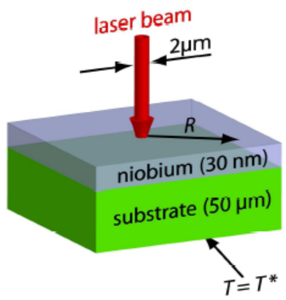

Pb

$BaFe_{12}0_{19}$

R. Werner, A.Yu. Aladyshkin *et al.*, Phys. Rev. B **84**, 020505(R) (2011).

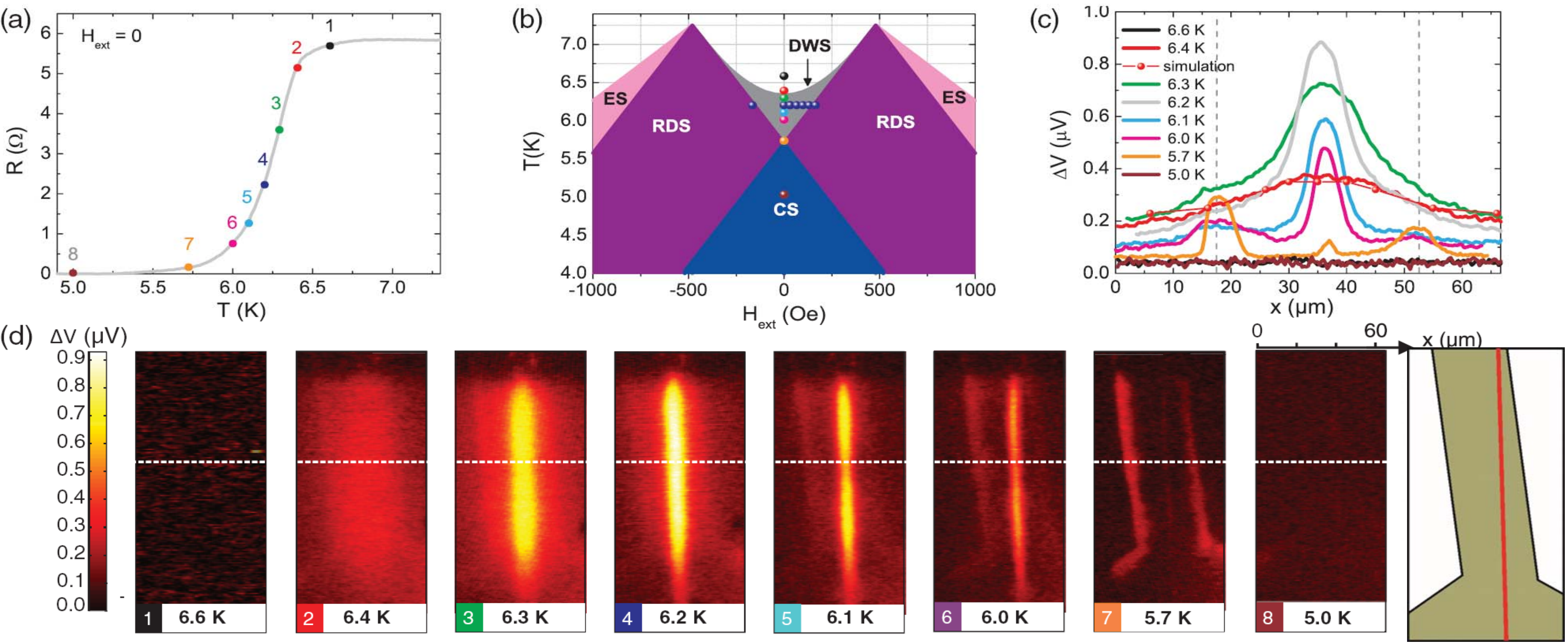

Vortex states

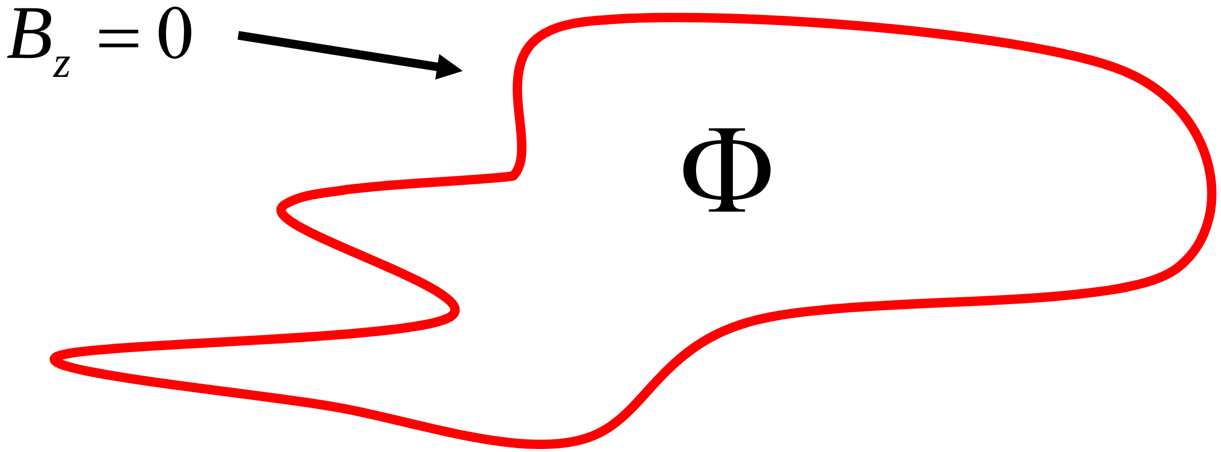

Superconducting films with arrays of ferromagnetic dots

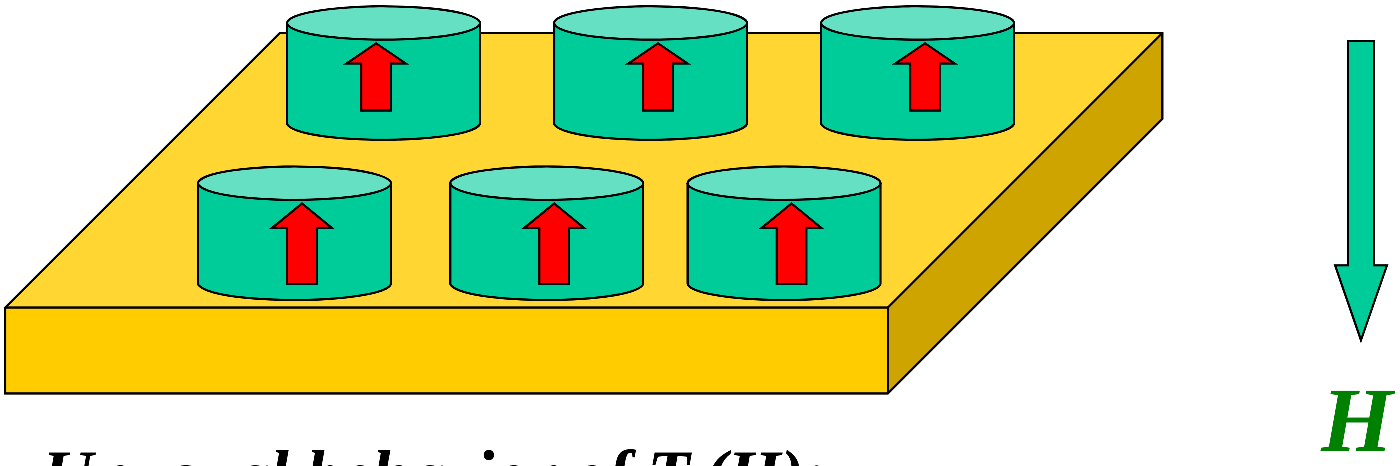

Unusual behavior of $T_c(H)$:

Y.Otani, B.Pannetier, J.P.Noziers,
D.Givord (1993)

Tc(H) oscillations

Nb-Gd/Co

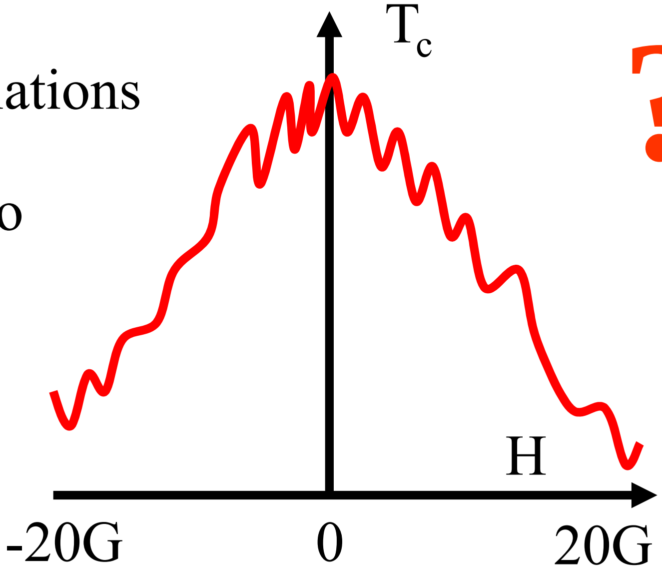

W.Gillijns, A. Silhanek,
V.Moshchalkov (2006)

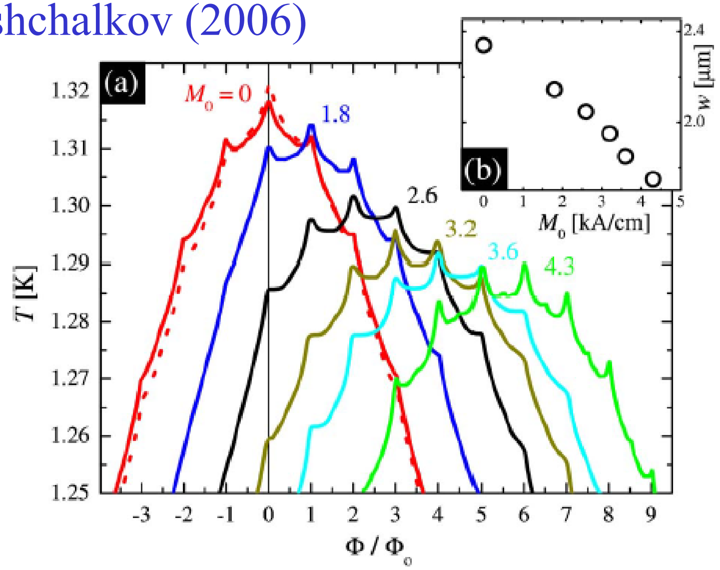

FIG. 2. (Color online) (a) Superconducting transition $T_c(H)$ of the Al film for different magnetic states of the dots. By increasing the magnetization a clear shift of $T_c(H)$ and a decrease of T_c^{max} is observed. (b) Lateral dimension w of the nucleation of superconductivity as a function of the magnetization of the dots.

Little-Parks effect and multiquanta vortices in a hybrid S/F system
Axially symmetric field profile

Example: magnetic dot (dipole) above S film

Superconducting ring with area S
Winding number=m

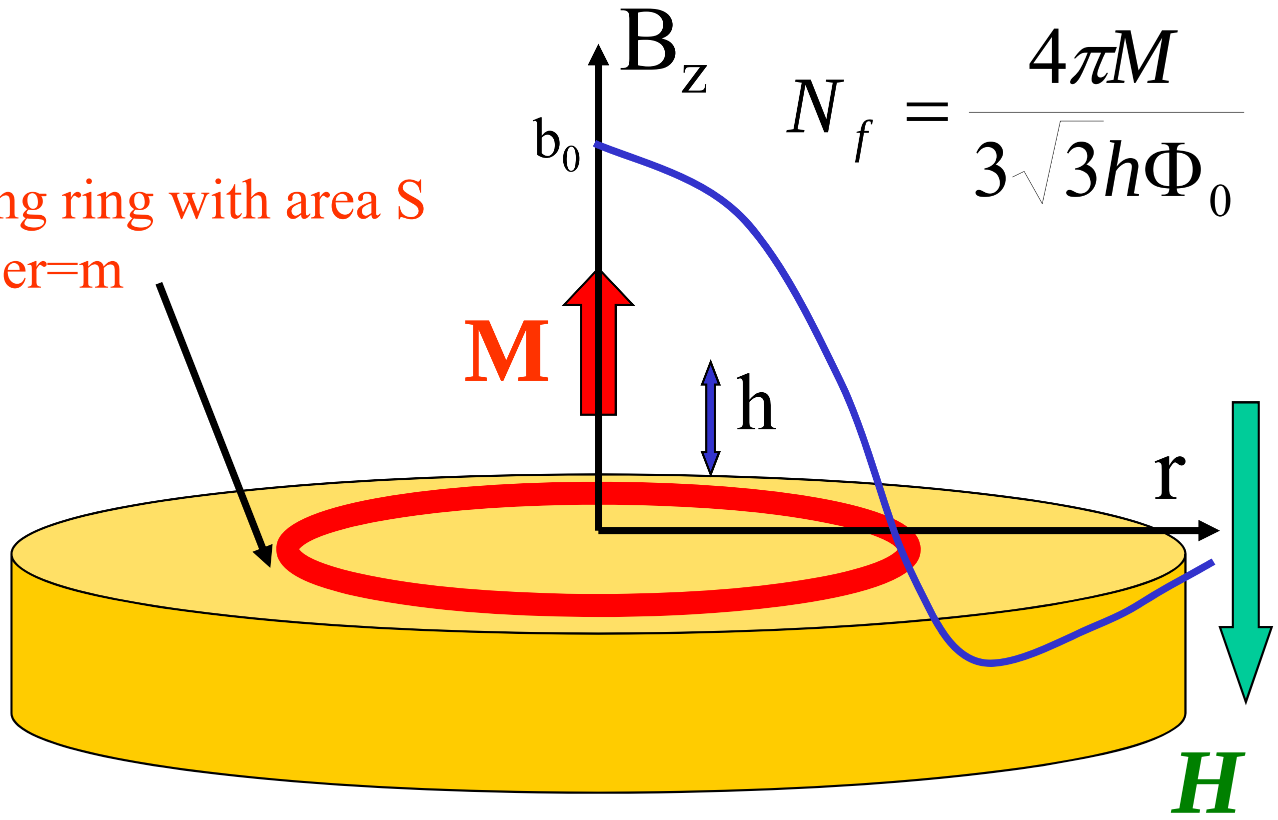

T_c (H) oscillations are caused by the quantization of flux through the area S

Magnetic dot assisted superconductivity.
T_c oscillations for a nucleus at the ring

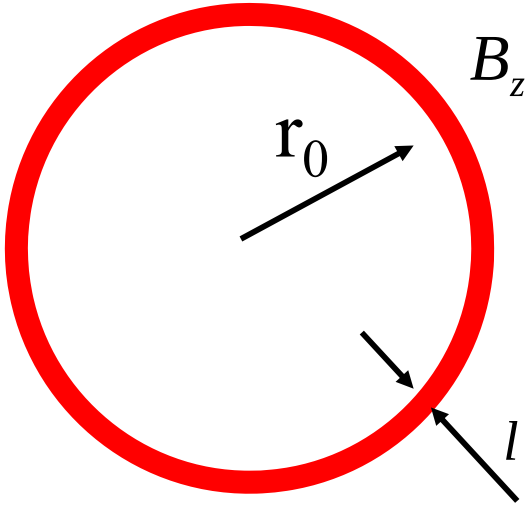

$$B_z(r_0) = 0$$

Local approximation: $l << r_0$

S nucleus in a linear B profile

$$l = \sqrt[3]{\frac{\Phi_0}{\pi \, | B_z'(r_0) |}}$$

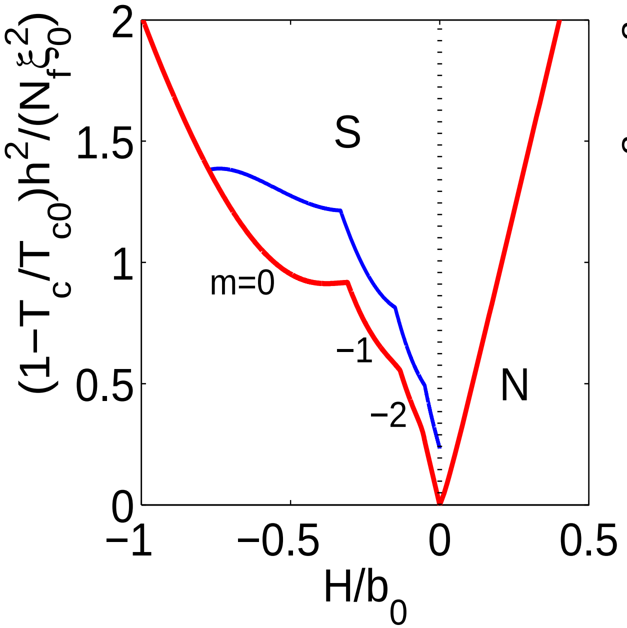

$N_f = 4$

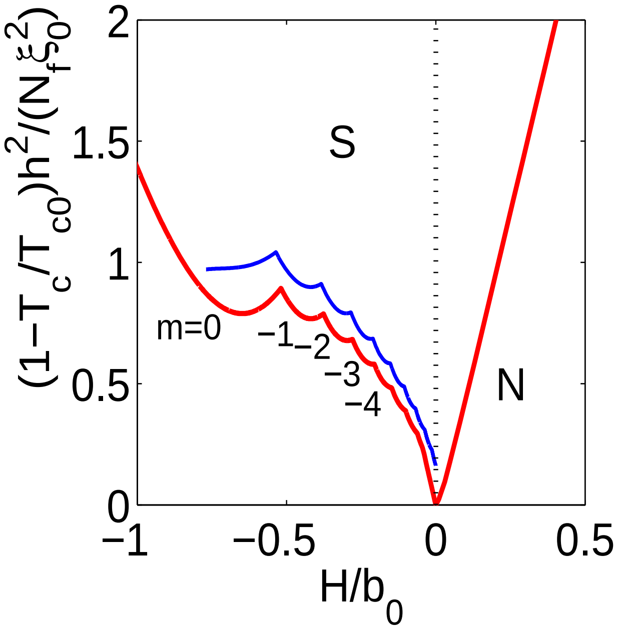

$N_f = 10$

F particle 300 x 300 x 300 nm,
magnetization ~ 10^3 G,
h~300 nm

$$M \sim 3 \cdot 10^{-11} G \cdot cm^3$$

$$b_0 \sim 10^3 G \qquad N_f \sim 10$$

Nb film: $T_{c0} \sim 9K$

$$\xi_0 \sim 40\, nm$$

$$\Delta H \sim 100\, G$$

$$\Delta T_c \sim 0.1 K$$

Interaction of domain structures with superconducting phase far below the superconducting transition (SF bilayers)

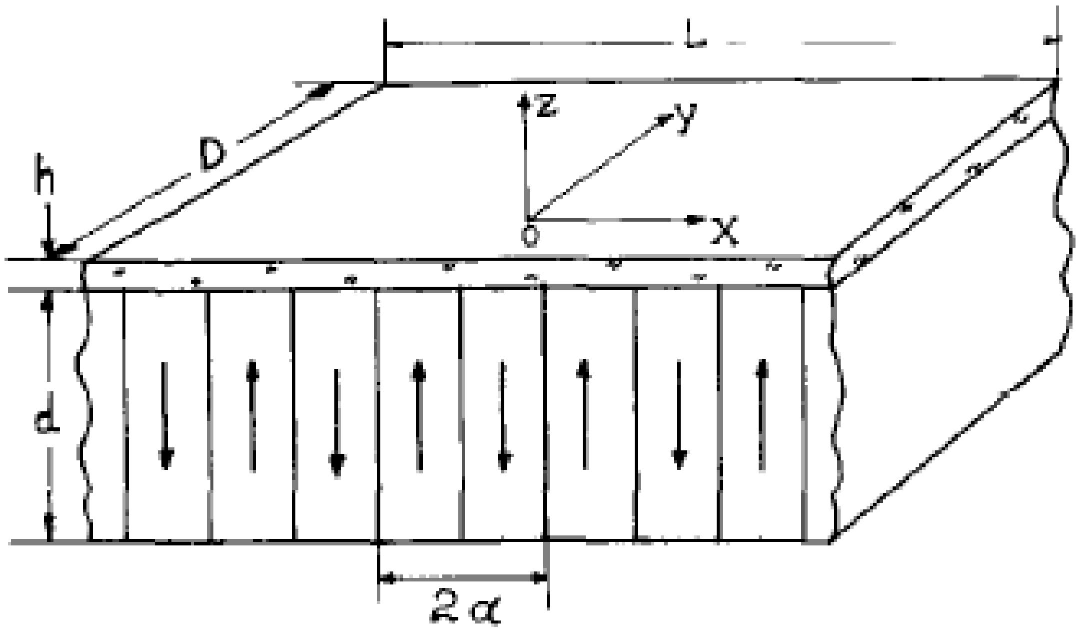

1. Meissner state
2. Penetration of the first vortex
3. Vortex-antivortex structures

Interaction of domain structures with superconducting phase far below the superconducting transition (ferromagnetic superconductors)

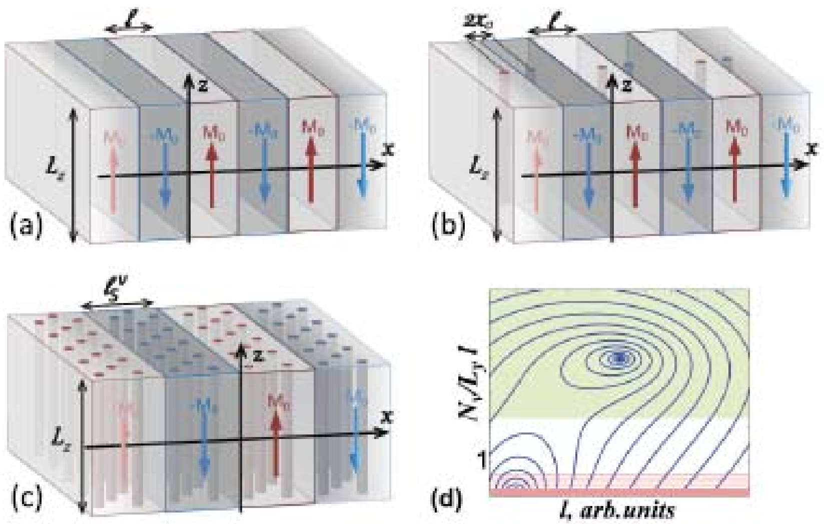

FIG. 1. (Color online) (a)–(c) The sketch of the magnetic domain structure in the ferromagnetic superconductor of the thickness $2L_z$ with the stripe structure of the domains with the size l: (a) in the Meissner state; (b) in the vortex state with one vortex (or antivortex) in each domain with the distance x_0 between each of them and the nearest domain wall; (c) in the vortex state with the dense vortex lattice. (d) The sketch of the applicability of the model at the diagram of the domain size l and the vortex number N_V/lL_y in each domain. The horizontal red solid line corresponds to the Meissner-state results, the cross-hatched region near the horizontal axis stands for calculations of the Bean-Livingston barrier profile and the vortex penetration threshold, and the green (shaded) region corresponds to the validity of the dense vortex lattice results. The contour plot of the total energy is drawn by blue curves.

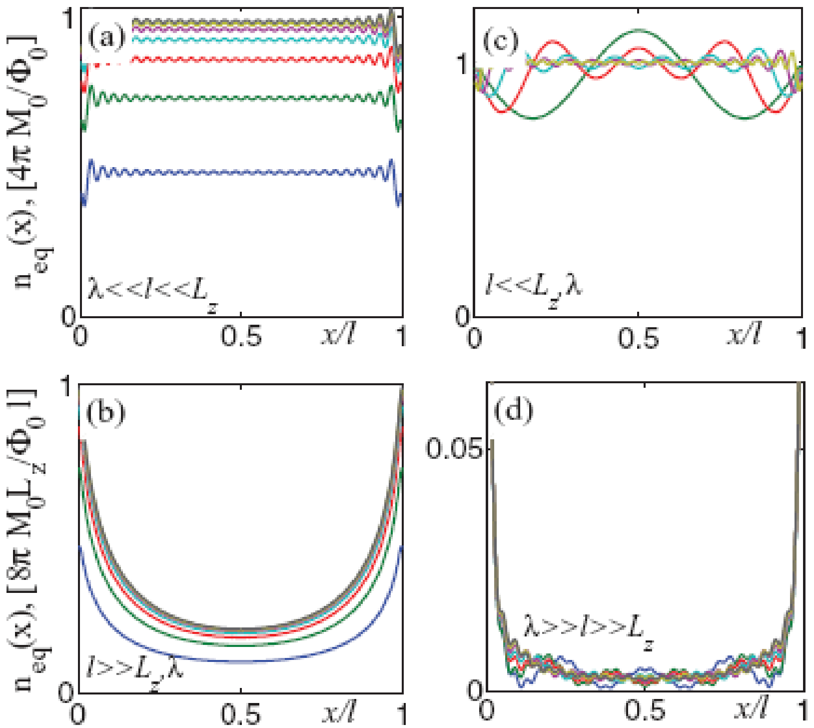

FIG. 3. (Color online) The space profiles of the vortex density distribution function for the different parameter values: (a) $l_v = 10^{-4}L_z$, $l = 0.01L_z$, (b) $l_v = 0.01L_z$, $l = 10L_z$; the plots at panels (a) and (b) from bottom to top correspond to the increasing ratio λ/l_v from the threshold value $2^{-3/2}$ to the 10th higher value; (c) $l_v = 10^{-4}L_z$, the plots from bottom to top correspond to the increasing ratio l/l_v from the value 1.6 to the value 10; (d) $l_v = 3L_z$, the plots from bottom to top correspond to the increasing ratio l/l_v from the value ~80, where $n_{eq}(x)$ becomes positive, to the 10th higher value. Note that plots at panels (c) and (d) remain intact for any $\lambda \gg l$.

Skyrmions (cylindrical magnetic domains) in SF bilayers. Metastable states at antidots

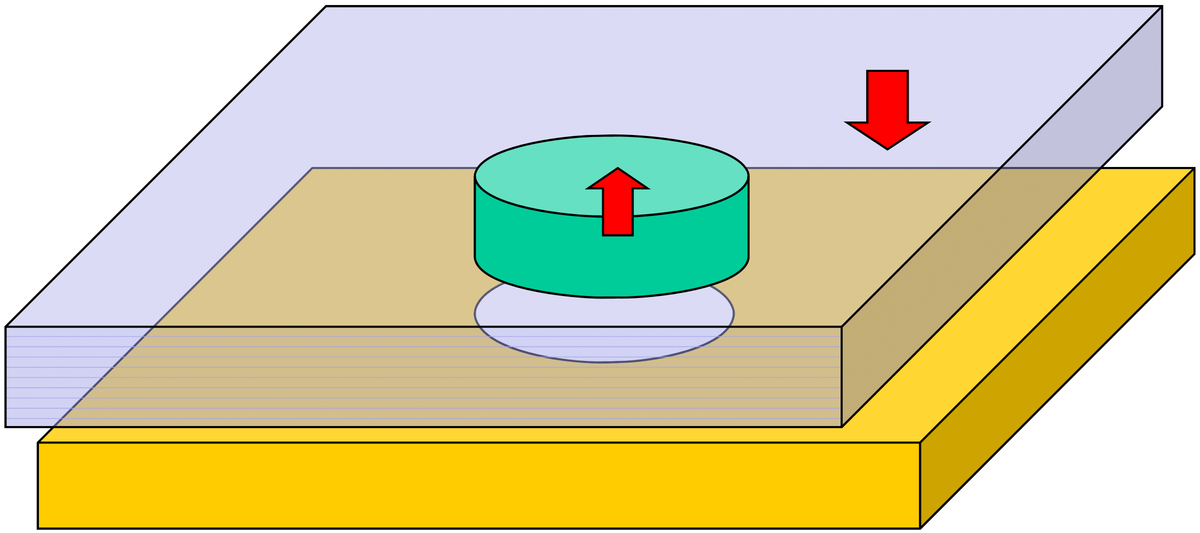

Vortices in superconductor-ferromagnet systems

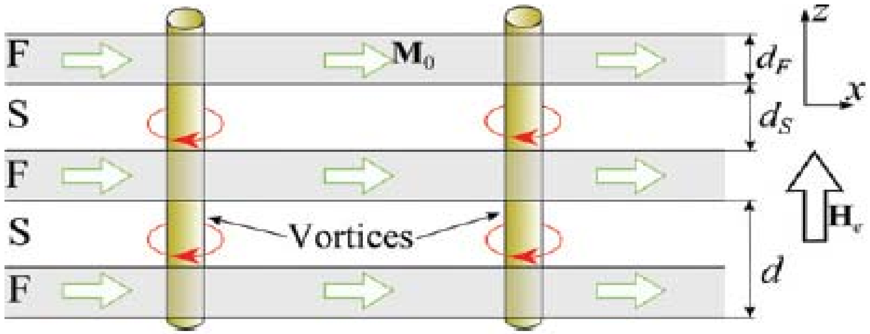

Fig. 1: (Colour on-line) Vortex lines in the SF superlattice with codirectional magnetic moments M_0 in all layers.

Vortex attraction: modulated vortex concentration

Moving vortex generates magnons

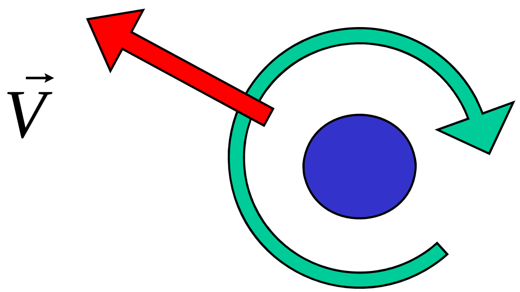

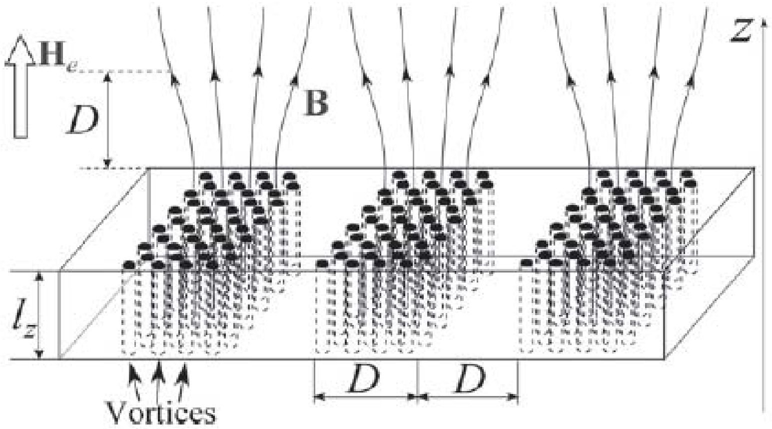

Fig. 5: A schematic picture of the stripe domain structure in the intermediate mixed state of the SF system at $H_{ez} \approx B_{0z}(H_{c1})/2$.

Josephson transport in the field of magnetic particles

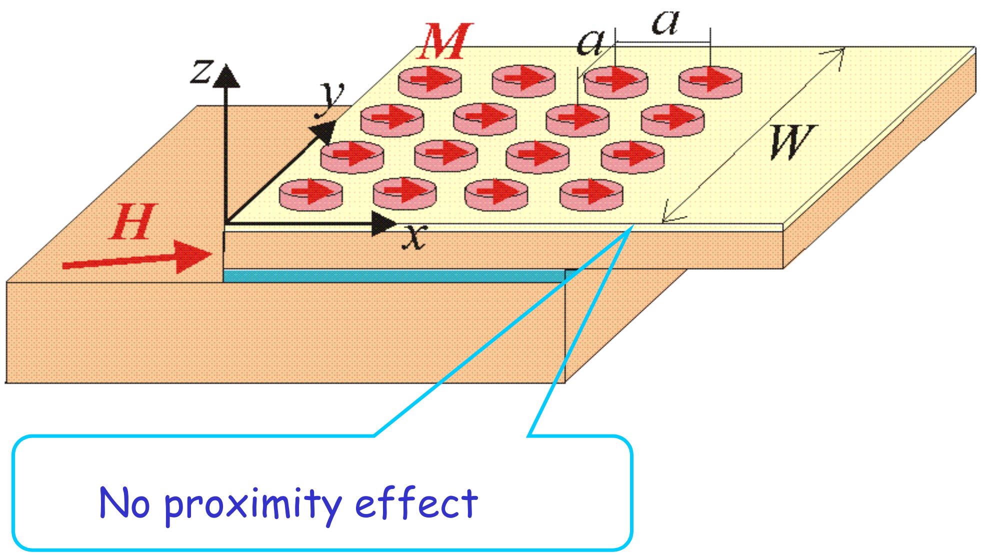

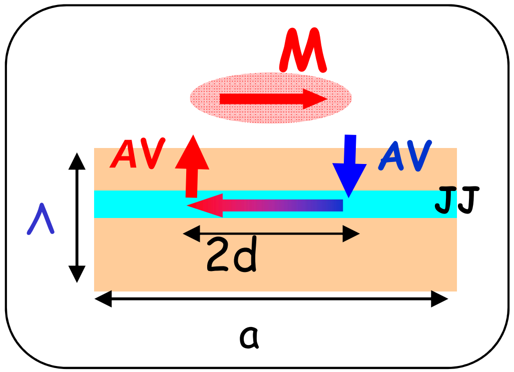

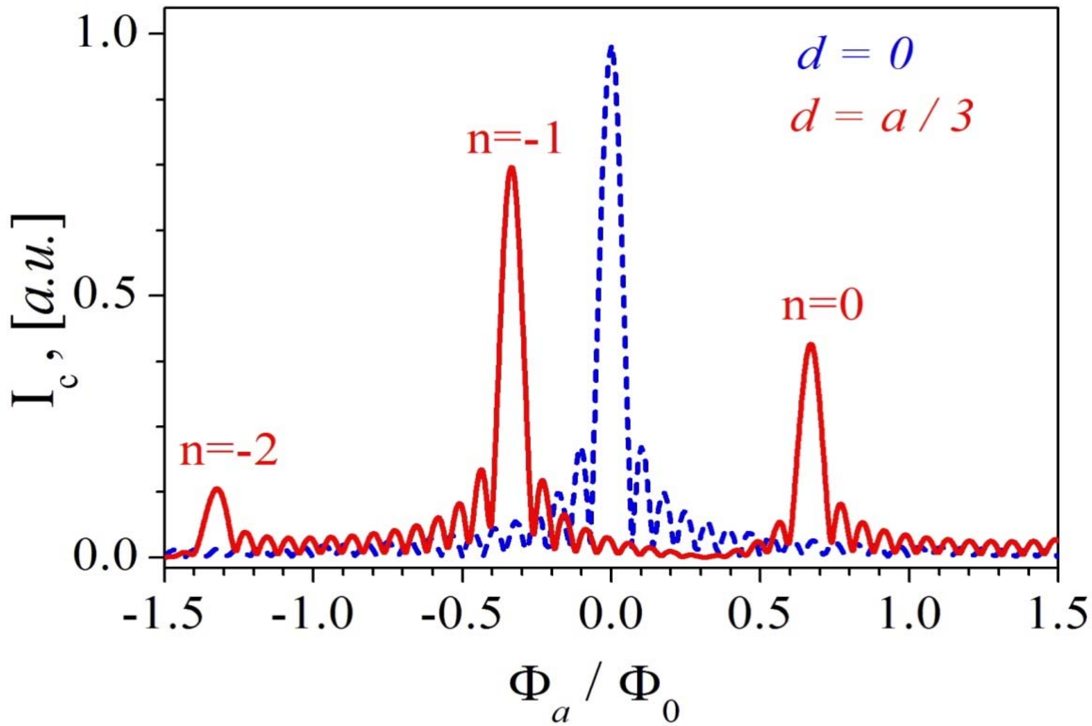

$$H = H_a\,(n + 2d/a)$$

$$\Phi_a = \Phi_0\,(n + 2d/a)$$

What is the electromagnetic response of superconductor and ferromagnet? Microscopic consideration.

London equation

$$\vec{j} = -\frac{e^2 n_s}{mc}\vec{A}$$

Exchange mechanism. Proximity effect in FS structures.

Question: Is it possible to affect vortex states by the exchange field?

$$\delta\hat{H} = \vec{h}\,\hat{\vec{\sigma}}$$

Inhomogeneous superconductivity induced by the exchange field:

1. FFLO state

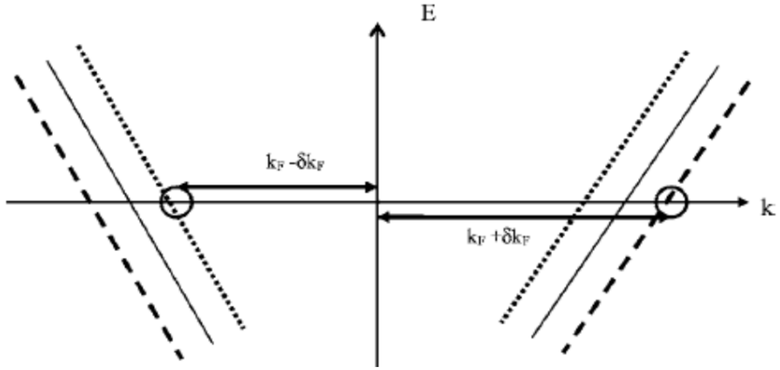

2. Interference effects for Cooper pairs in FS layered structures

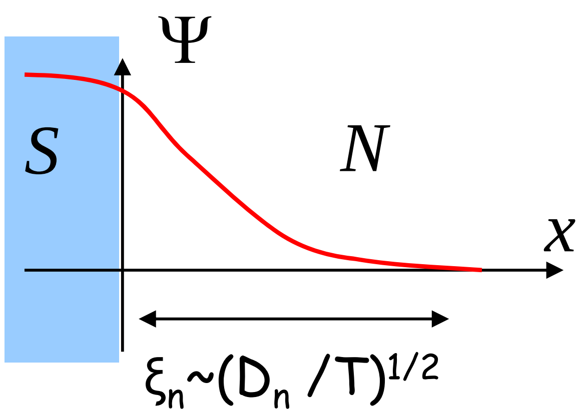

Damped oscillatory dependence of pair wave function in ferromagnets

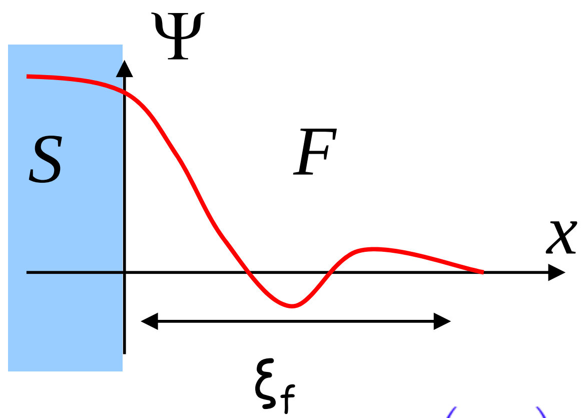

h= exchange energy

$$\Psi \sim \Delta \exp\left(-\frac{x}{\xi_f}\right) \cos\left(\frac{x}{\xi_f}\right)$$

in dirty limit: $\xi_f = \sqrt{\dfrac{D_f}{h}}$

Spontaneous currents in S/F bilayers. Inverse proximity effect.

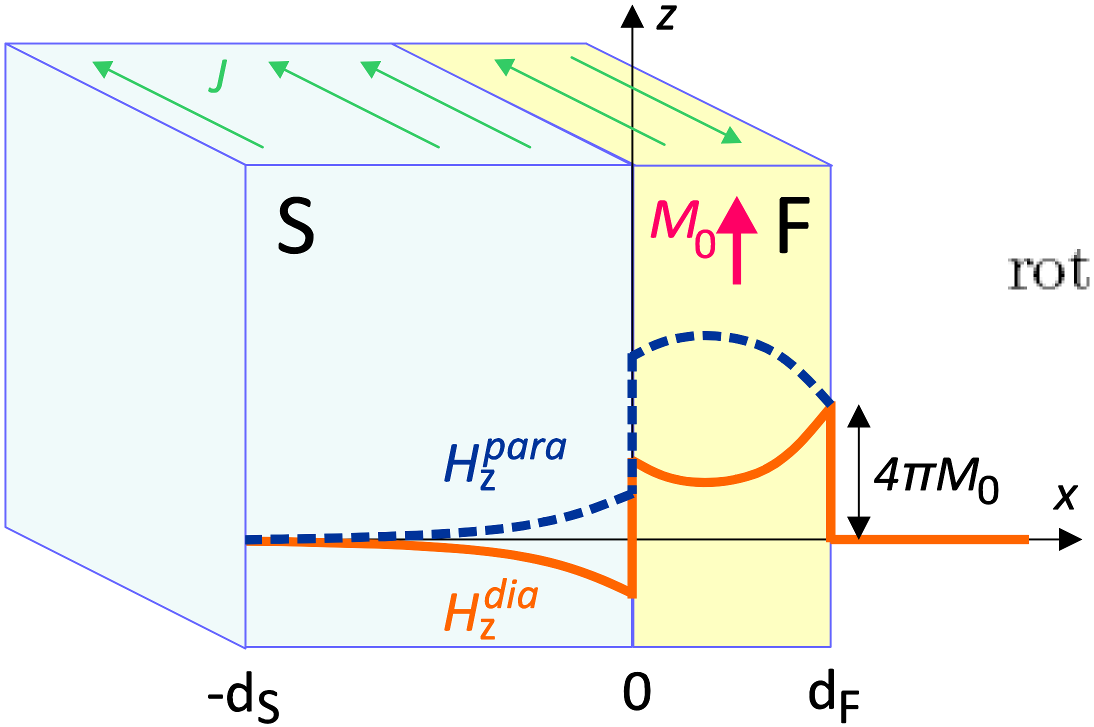

$$\mathrm{rot\ rot}\,\mathbf{A} = \frac{4\pi}{c}\left(\mathbf{j}_s + \mathbf{j}_m + \mathbf{j}_{surf}\right)$$

$$B_z = -\frac{4\pi M_0 Q}{\sinh\left(d_s/\lambda\right)} \sinh\left(\frac{x+d_s}{\lambda}\right)$$

Manifestation of proximity effect in electrodynamic response

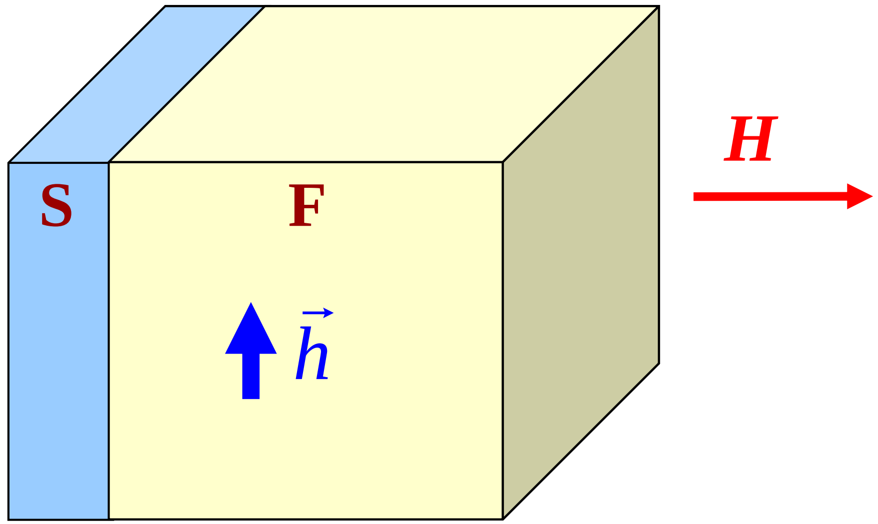

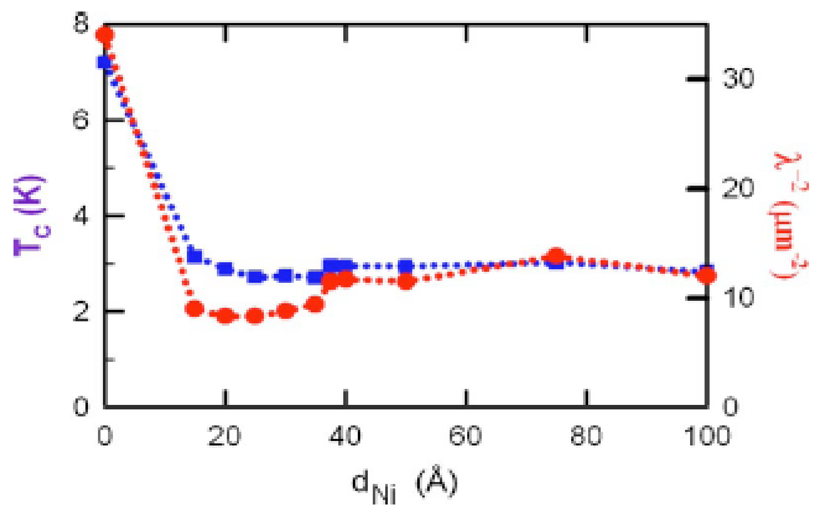

FIG. 2. (Color online) T_C (squares) and $\lambda^{-2}(0)$ (circles) vs d_{Ni} for Nb/Ni bilayers with d_{Nb}=102 Å.

London penetration depth of S/F bilayers

Experiment :
Lemberger et al. , J. Appl. Phys. (2008).
Measurable quantity:
integrated (over the system thickness) screening length.

Theory :
Houzet, Meyer, PRB (2009).
Slightly non–monotonous dependence of λ^{-2} vs d_F

Screening properties of Nb/PdNi/Nb

H = 0

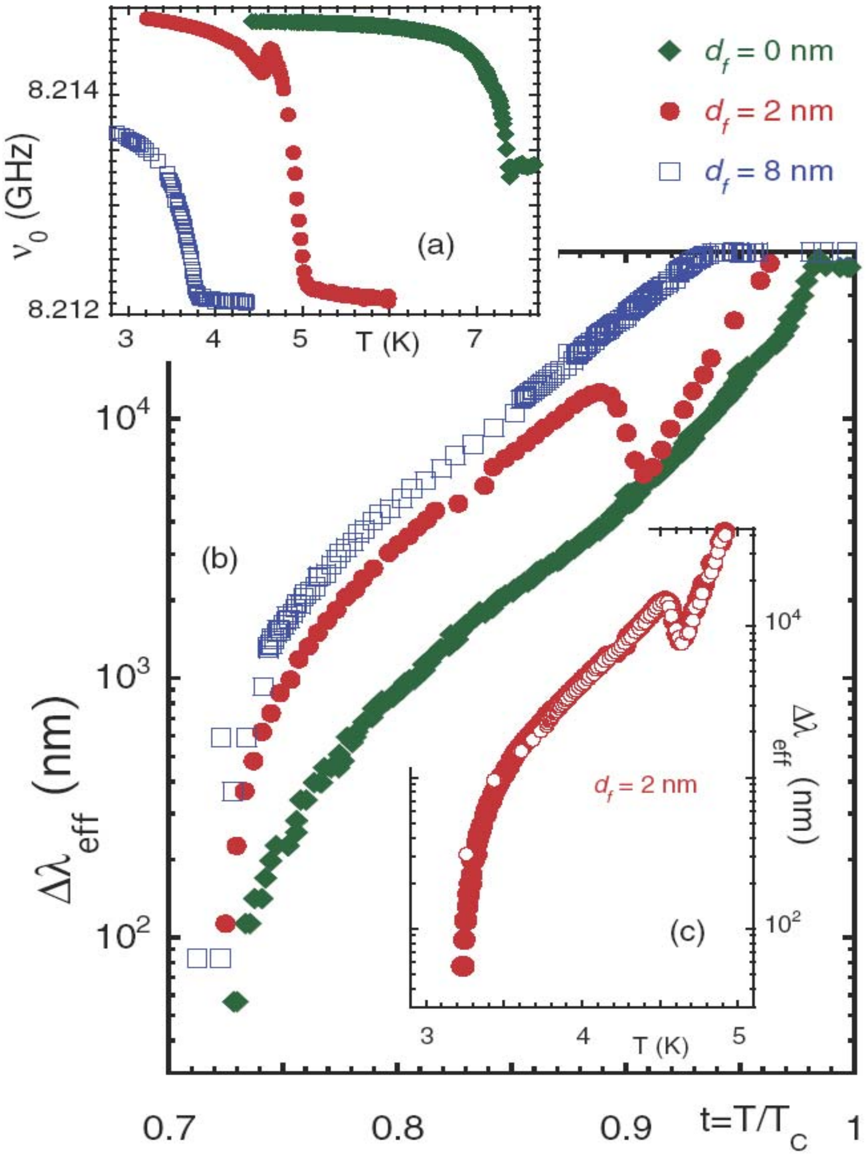

Nonmonotoneous behavior o $\Delta\lambda_{\mathrm{eff}}(T)$

Transition between 0 and π - states ?

N.Pompeo, et al., PRB 90, 064510 (2014)

Screening properties of SFS structures

$$F_{GL}^{0,\pi}(T) = E_0 \left[a^{0,\pi} \frac{T - T_c^{0,\pi}}{T_c^{0,\pi}} \Delta^2 + \frac{b^{0,\pi}}{2} \Delta^4 \right]$$

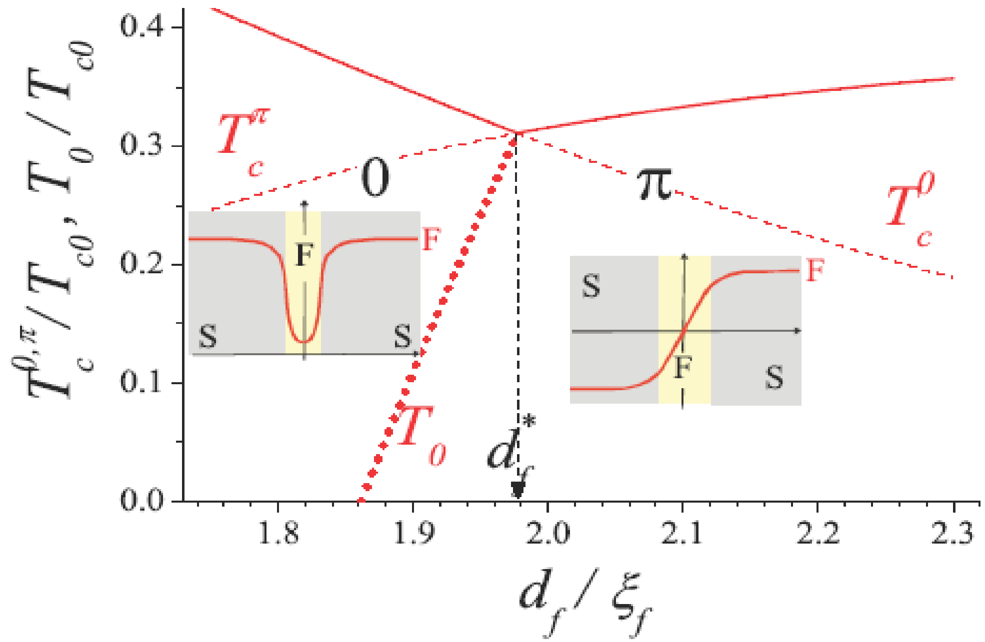

$$F^0(\Delta_0) = F^\pi(\Delta_\pi) \qquad \frac{T_c^0 - T_0}{T_c^\pi - T_0} = \frac{a^\pi T_c^0}{a^0 T_c^\pi} \sqrt{\frac{b^0}{b^\pi}}$$

$$\Delta_\pi^2(T_0) = \frac{a^\pi}{b^\pi} \left(\frac{T_c^\pi - T_0}{T_c^0} \right) = \Delta_0^2(T_0) \sqrt{\frac{b^0}{b^\pi}}$$

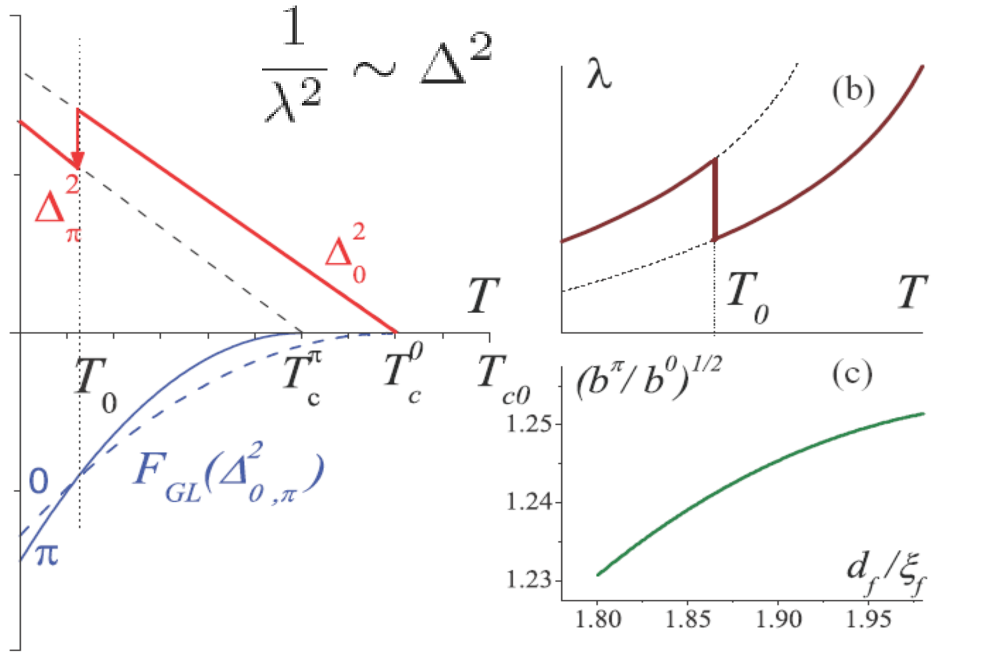

N.Pompeo, et al., PRB 90, 064510 (2014)

$Nb/Pd_{0.84}Ni_{0.16}/Nb$

<u>0-π переход I рода:</u>

A.I. Buzdin PRB 2005 (диффузионная SFS, "жесткие" гран. условия)

P.H. Barsic, O.T. Valls and K. Halterman, PRB2006 (баллистическая SFS система)

<u>Экранирующие свойства SF(S) структур</u>

T.R.Lemberger, et al JAP 2008

M. Houzet, J.S. Meyer, PRB 2009

S.Mironov, A.Melnikov, A.Buzdin, PRL 2012

$Nb/Cu_{0.35}Ni_{0.65}/Nb$

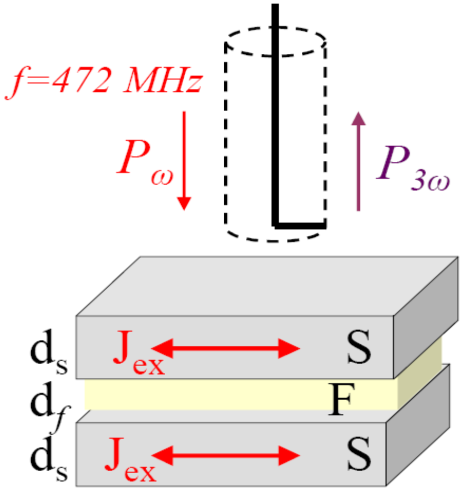

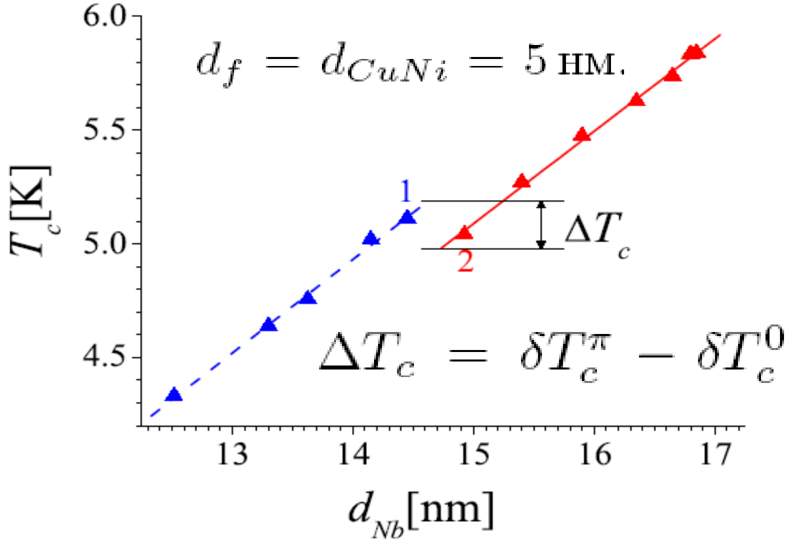

Рис.2 Зависимость критической температуры T_c от толщины S слоя d_{Nb} (▲) и её аппроксимация линейной функцией (сплошная и пунктирная линии).

[С.Н.Вдовичев, Е.Е.Пестов, Ю.Н.Ноздрин, П.А.Юнин]

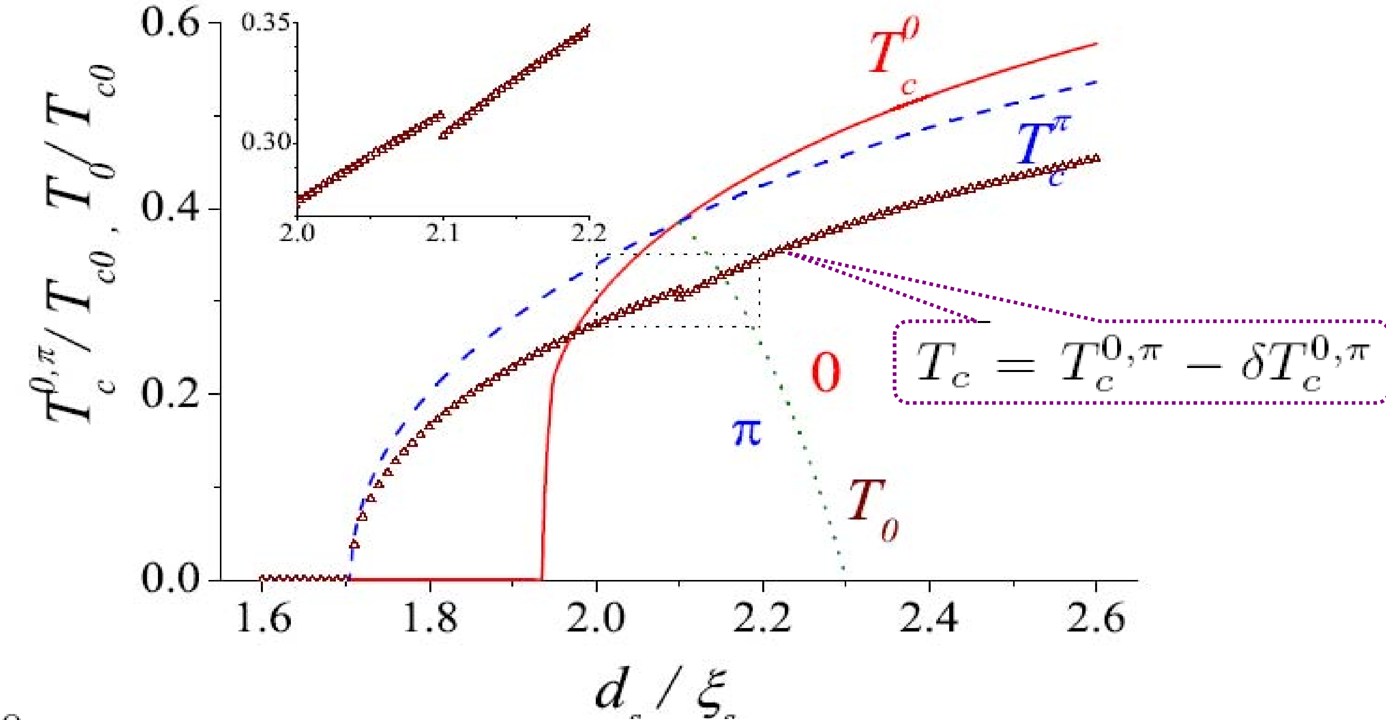

$$j_c^{0,\pi}(T) = j_{c0}\frac{(a^{0,\pi})^{3/2}}{b^{0,\pi}}\left(\frac{T_c^{0,\pi}-T}{T_c^{0,\pi}}\right)^{3/2}$$

$$j_{c0} = \frac{4\sqrt{2}eN(0)T_{c0}^{3/2}}{3\sqrt{3m}} . \quad (a^\pi)^{3/2}/b^\pi > (a^0)^{3/2}/b^0$$

$$j_{ex} = \begin{cases} j_c^\pi(T_c), & d_s < d_s^* \\ j_c^0(T_c), & d_s \geq d_s^* \end{cases} \Rightarrow T_c = T_c^{0,\pi} - \delta T_c^{0,\pi}$$

Paramagnetic Meissner effect in dirty S/F bilayers

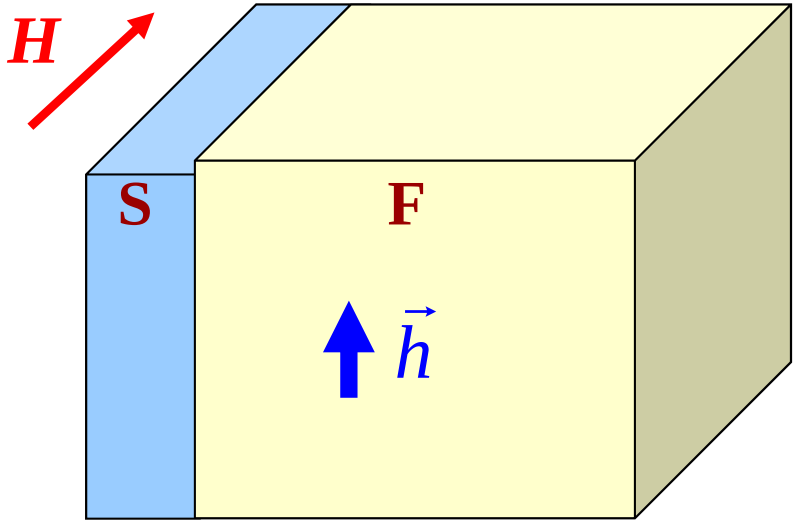

$$\vec{j} = -\frac{1}{4\pi}\lambda^{-2}\vec{A}$$

$$\lambda^{-2} = \frac{16\pi^2 T_c}{d_0}\sum_{n=0}^{\infty}\int \sigma\left(|f_s|^2 - |\vec{f}_t|^2\right)dx$$

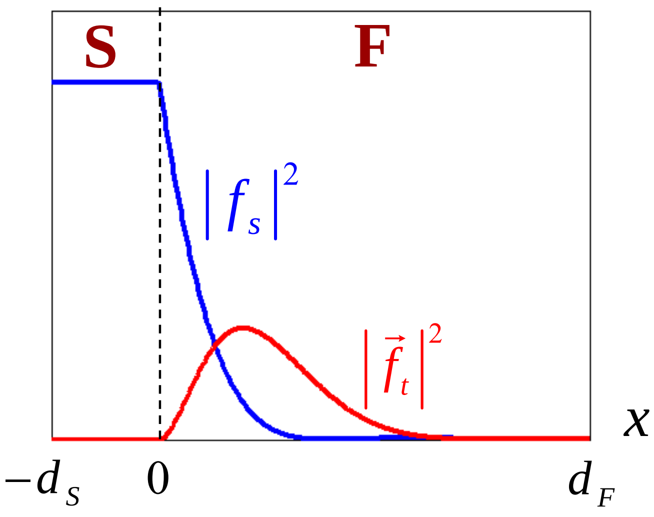

$$|\vec{f}_t|^2 > |f_s|^2 \Rightarrow \lambda^{-2}(x) < 0$$

local paramagnetic Meissner effect

Can the superfluid density change its sign?

$$\hat{f} = \left(f_s + \vec{f}_t\hat{\vec{\sigma}}\right)i\hat{\sigma}_y$$

Paramagnetic Meissner effect and the FFLO instability

$$\vec{j} = -\frac{1}{4\pi}\lambda^{-2}\vec{A} = -\frac{\delta F_A}{\delta \vec{A}} \quad \Longrightarrow \quad F_A = \frac{1}{8\pi}\int \lambda^{-2}\vec{A}^2 dV$$

$$F_A = \int \Lambda\left(\vec{A} - \frac{\Phi_0}{2\pi}\nabla\varphi\right)^2 dV$$

$$\Downarrow \quad \vec{A} = 0$$

$$F_A = \int \Lambda\left(\frac{\Phi_0}{2\pi}\nabla\varphi\right)^2 dV \qquad \lambda^{-2} = \frac{4\pi e^2 n_s}{m}$$

The uniform ground state can be unstable!

FFLO states in thin-film S/F systems

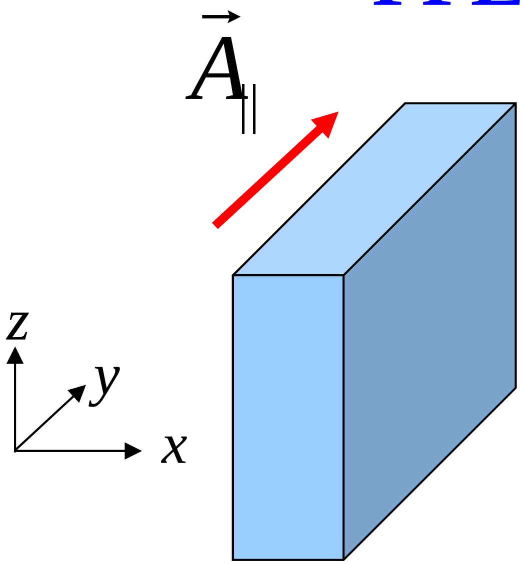

$d_0 << \lambda$

$$\hat{f} \propto e^{i\vec{k}\vec{r}}$$

$$F_A = \left(\vec{A}_{\parallel} - \frac{\Phi_0}{2\pi}\vec{k} \right)^2 \frac{S}{8\pi} \int \frac{dx}{\lambda^2}$$

A hallmark of the instability: vanishing Meissner effect

$$\lambda^{-2} = \frac{1}{d_0} \int \frac{e^2 n_s}{2m} dx < 0 \quad \Longrightarrow \quad \textbf{FFLO state}$$

FFLO state in S/F bilayers

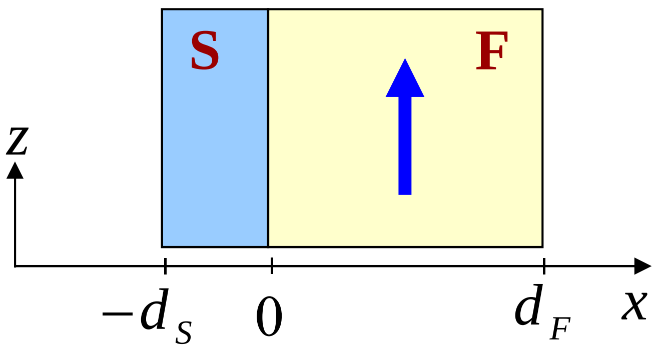

$$\frac{D}{2}\frac{\partial^2 \hat{f}}{\partial x^2}-\left(\omega_n+\frac{D}{2}k^2\right)\hat{f}-\frac{i}{2}\left(\vec{h}\hat{\vec{\sigma}}\hat{f}+\hat{f}\vec{h}\hat{\vec{\sigma}}\right)+\hat{\Delta}=0$$

$$\Delta\ln\frac{T_c}{T_{c0}}+\sum_{n=-\infty}^{\infty}\left(\frac{\Delta}{|2n+1|}-\pi T_c f_{12}^S\right)=0$$

Stability of the FFLO state:

$$d_F \sim \xi_f$$

$$\frac{h}{T_{c0}}\xi_f \le d_S \le \frac{D_f}{D_s}\xi_f$$

$$\frac{D_f}{D_s} >> \frac{h}{T_{c0}}$$

$$T_c << T_{c0}$$

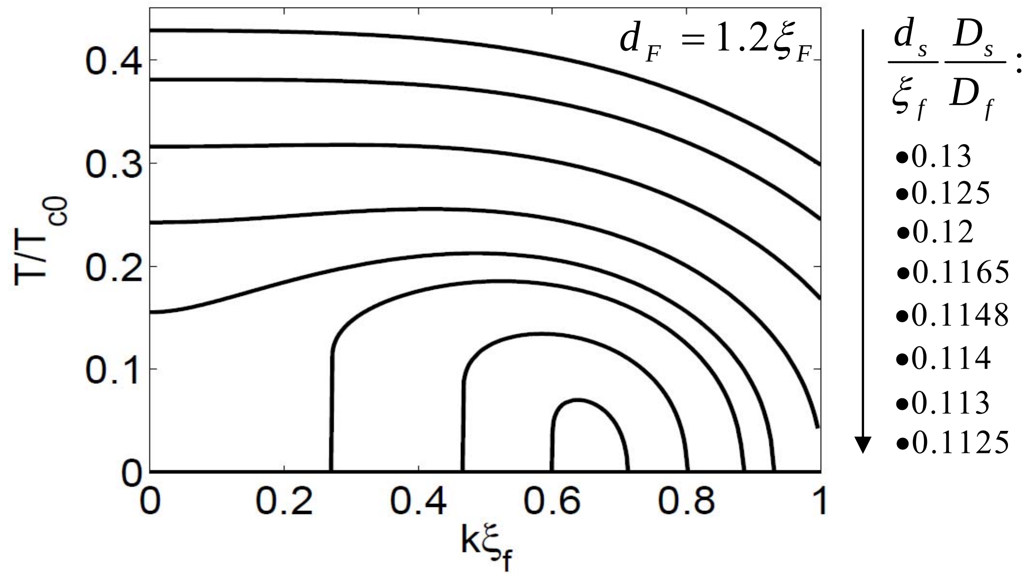

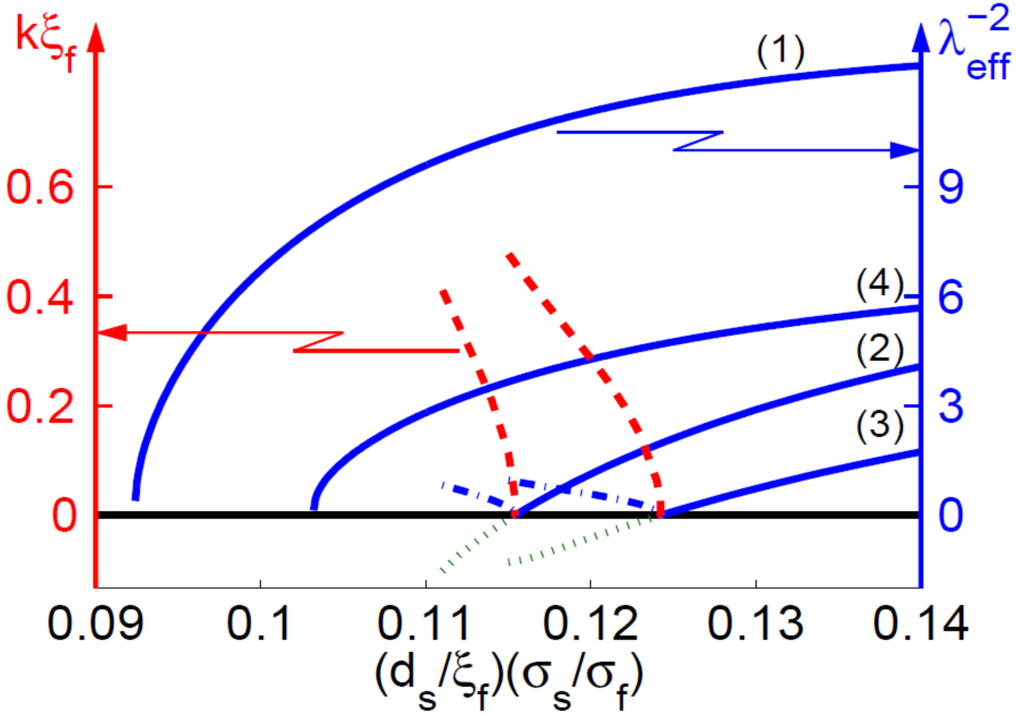

$$\lambda^{-2}=-\frac{16\pi^2 d_s\sigma_s\Delta^2}{ec\Phi_0 d_0 D_s T_c(0)}\left[1-\mathrm{Re}\left\{\nu\Psi_1\left(\frac{1}{2}+\nu\right)\right\}\right]\left.\frac{\partial T_c}{\partial(k^2)}\right|_{k=0}$$

Other systems with in-plane FFLO instability

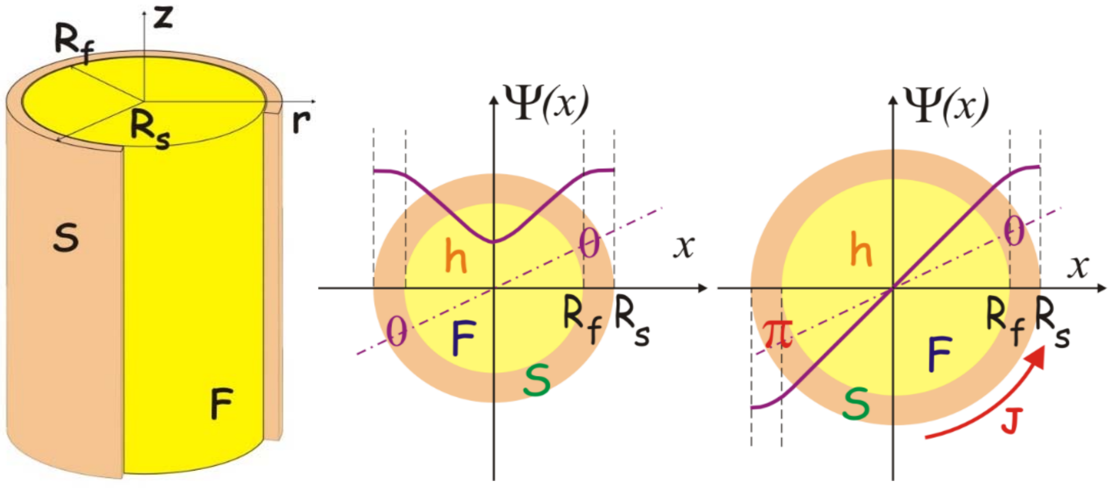

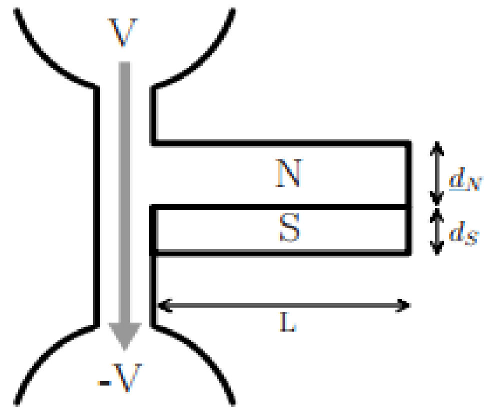

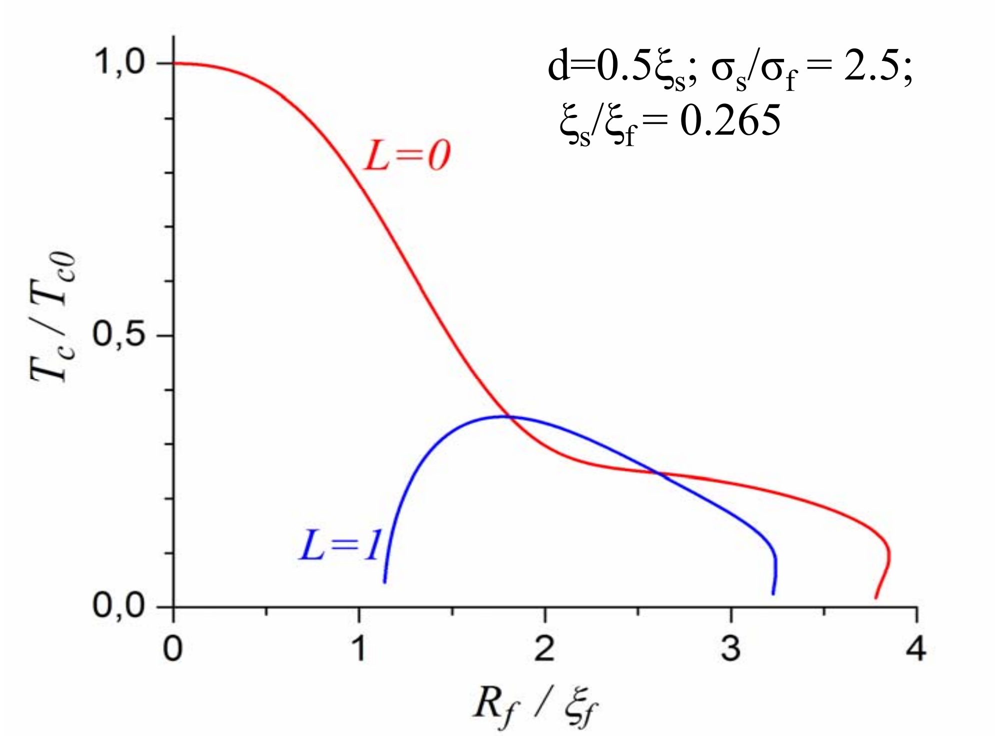

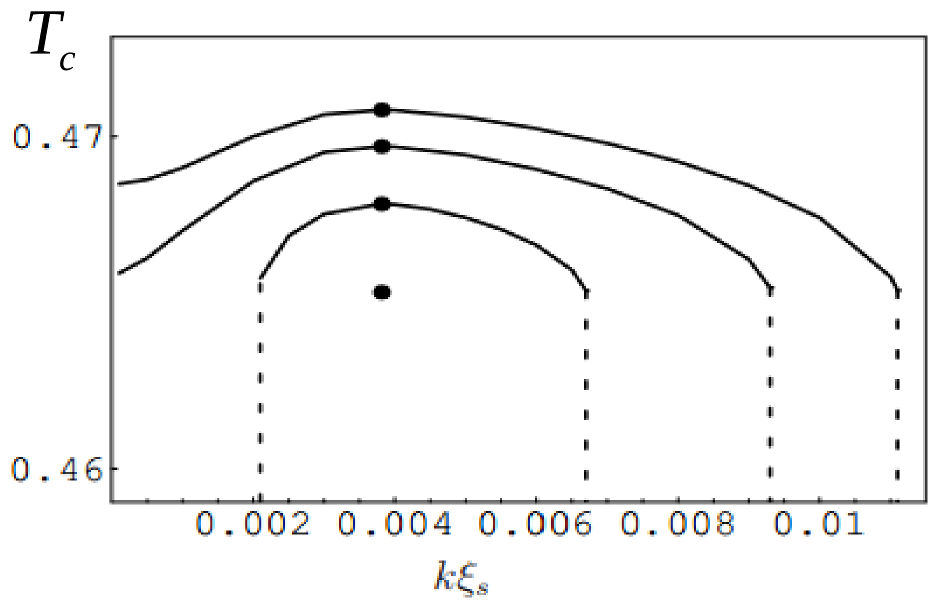

A.V. Samokhvalov, A.S. Mel'nikov and A.I. Buzdin, Phys. Rev. B **76**, 184519 (2007)

I.V. Bobkova and A.M. Bobkov, Phys. Rev. B **88**, 174502 (2013)

What happens below T_c?

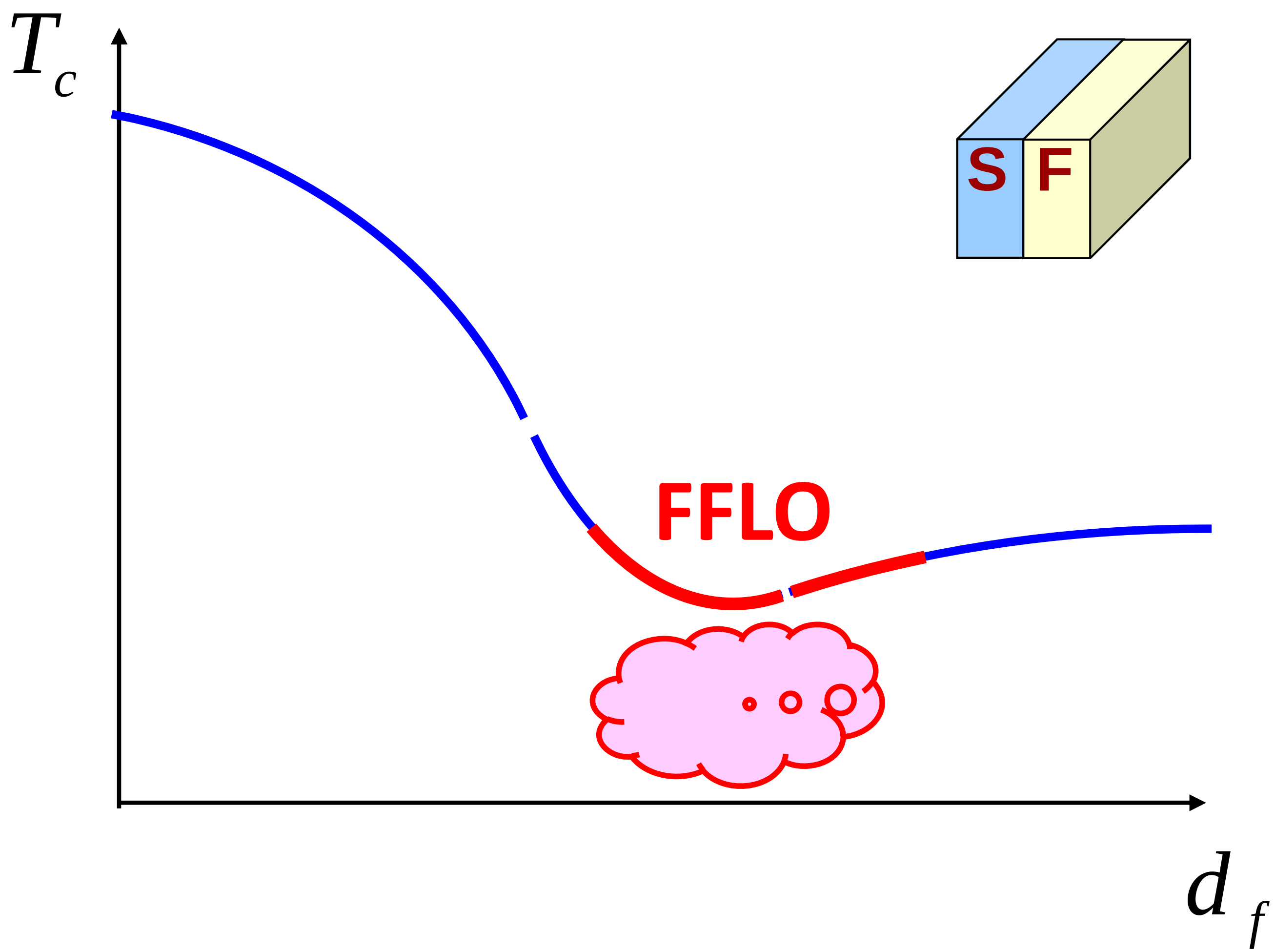

The idea about the low-temperature FFLO phase

$$\lambda^{-2}(T) = A(T_c - T) + B(T_c - T)^2 + \dots$$

$A < 0 \Longrightarrow$ **FFLO instability at T = T$_c$**

$A > 0 \Longrightarrow$ **No FFLO at all?**

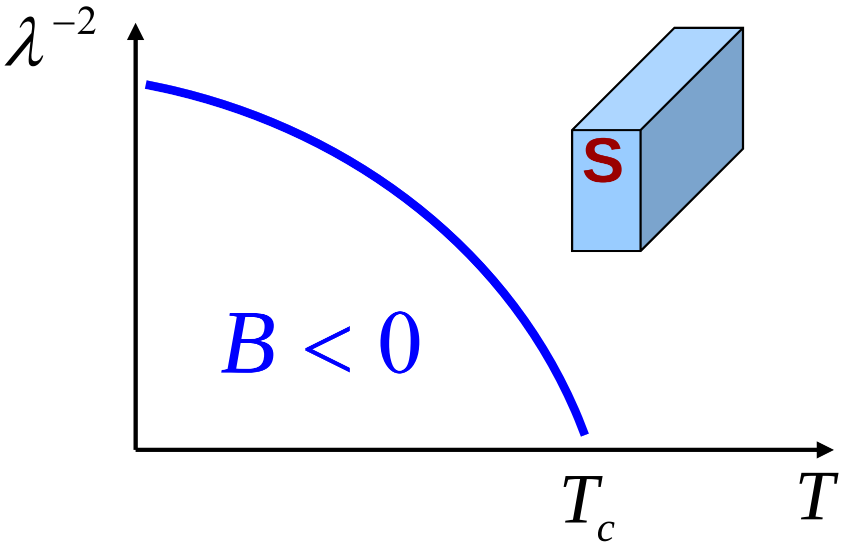

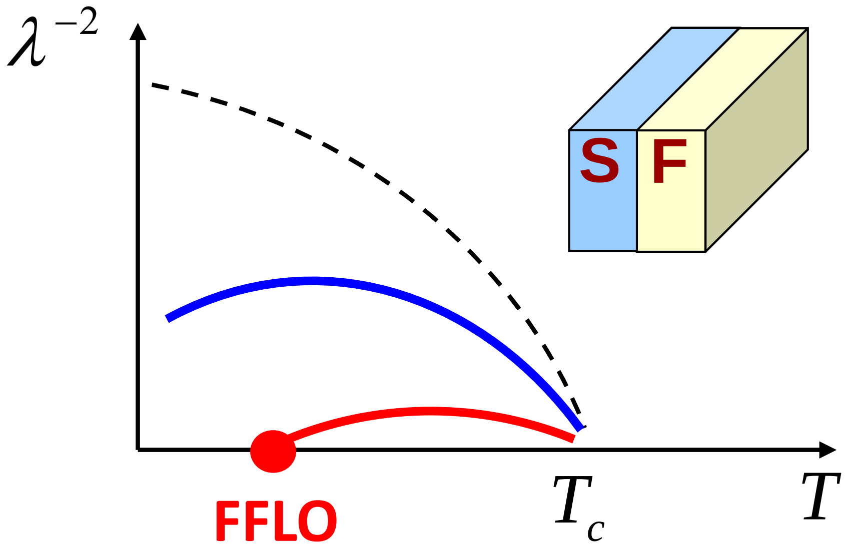

Analytical results

$$\lambda^{-2}(\Delta) = a\,\Delta^2(T) + b\,\Delta^4(T) + \ldots$$

$a > 0 \qquad b < 0 \quad \Rightarrow \quad$ FFLO instability at $\Delta^2(T) = \dfrac{a}{|b|}$

Nonlinear Usadel

⇩

$f_s(x) \quad f_t(x)$

A. V. Samokhvalov, A. I. Buzdin,
PRB **92**, 054511 (2015)

⇩

$$\lambda^{-2} = \frac{16\pi^2 T_c}{d_0} \sum_{n=0}^{\infty} \int \sigma \left(|\, f_s|^2 - |\, \vec{f}_t|^2 \right) dx$$

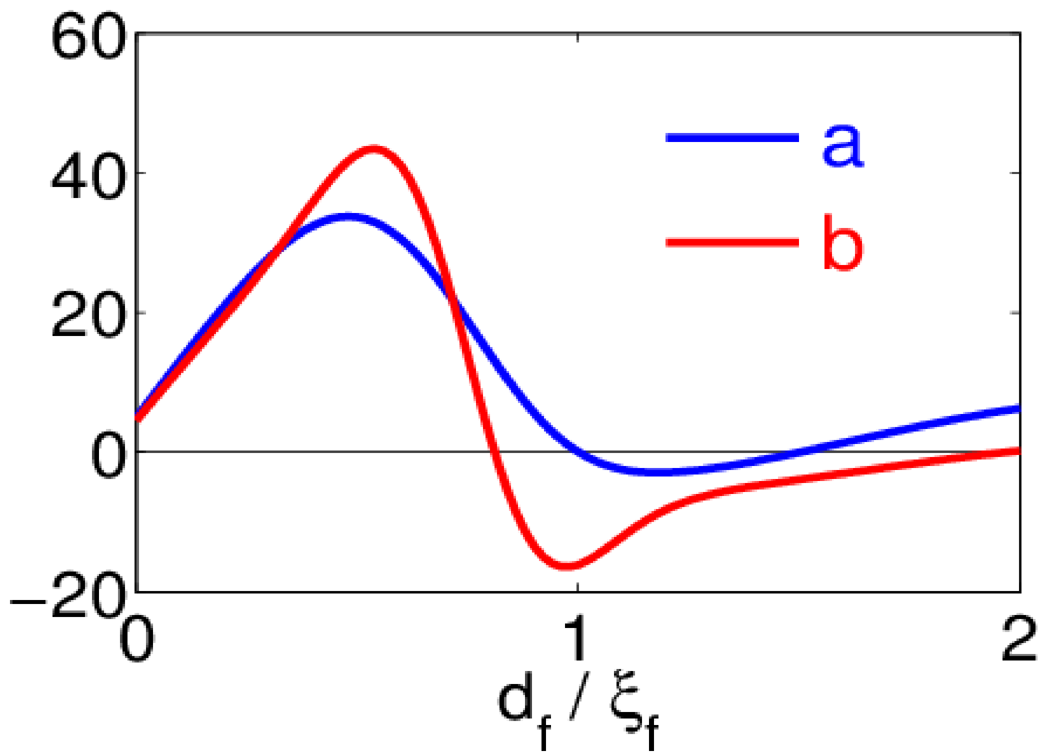

FFLO states in S/F/N structures

$$\lambda^{-2} = \frac{16\pi^2 T_c}{d_0} \sum_{n=0}^{\infty} \int \sigma \left(| f_s |^2 - | \vec{f}_t |^2 \right) dx$$

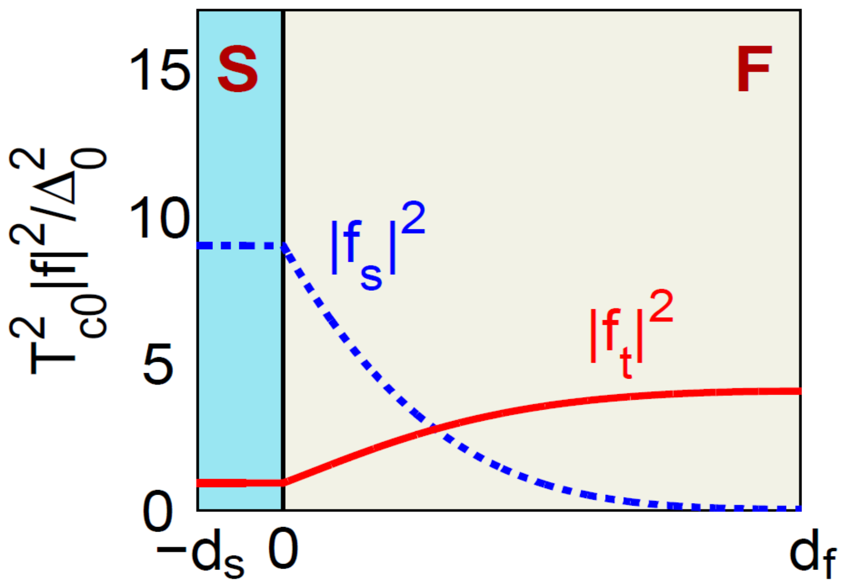

FFLO states in S/F/N structures

$$\lambda^{-2} = \frac{16\pi^2 T_c}{d_0} \sum_{n=0}^{\infty} \int \sigma \left(| f_s |^2 - | \vec{f}_t |^2 \right) dx$$

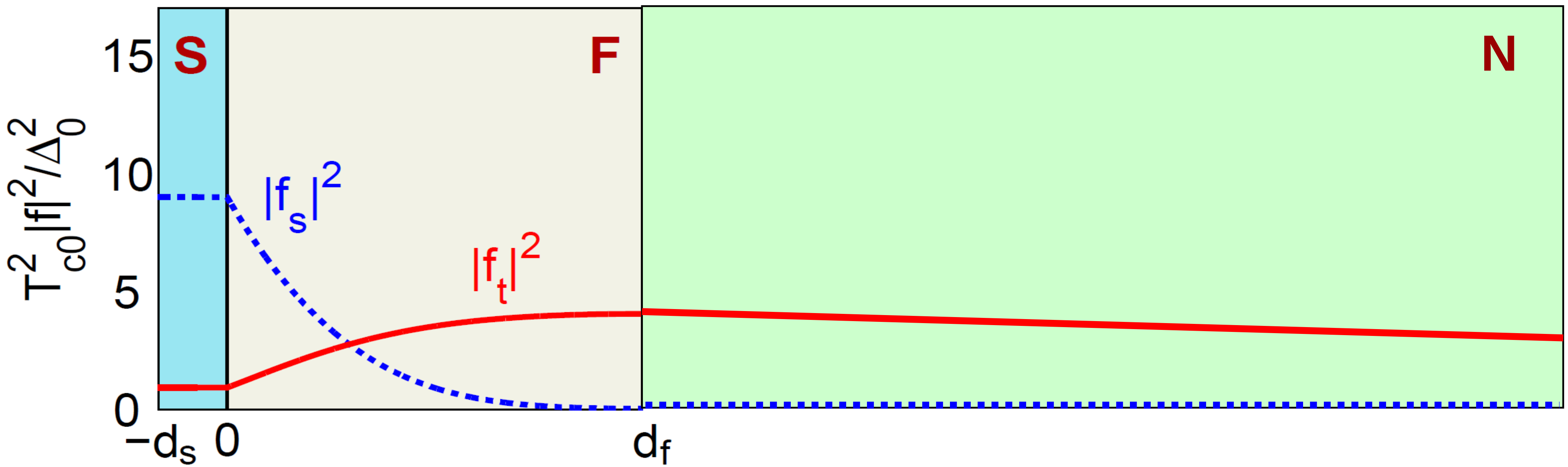

Phase diagrams of the superconducting films

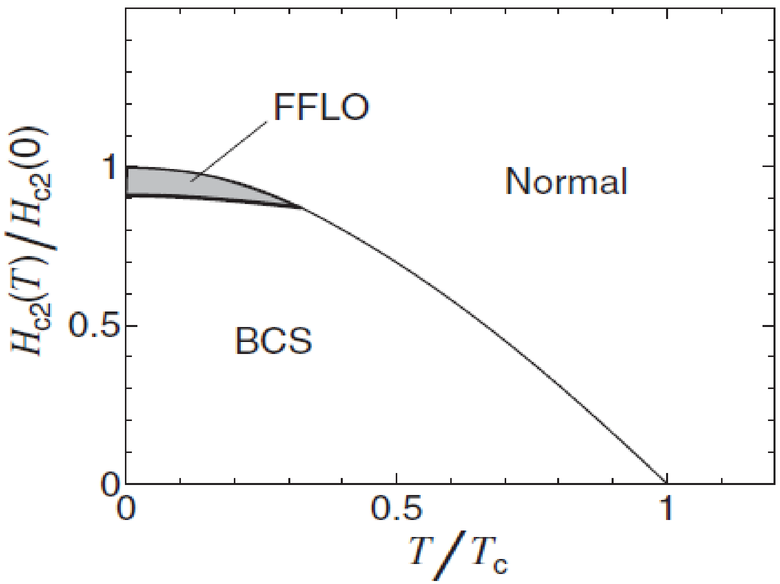

Fig. 5. H–T phase diagram in the presence of the orbital effect, as proposed in ref. 8. The transitions from the normal state to the FFLO and BCS states are of second order (solid line), while the transition from the FFLO state to the BCS state is of first order (thick solid line).

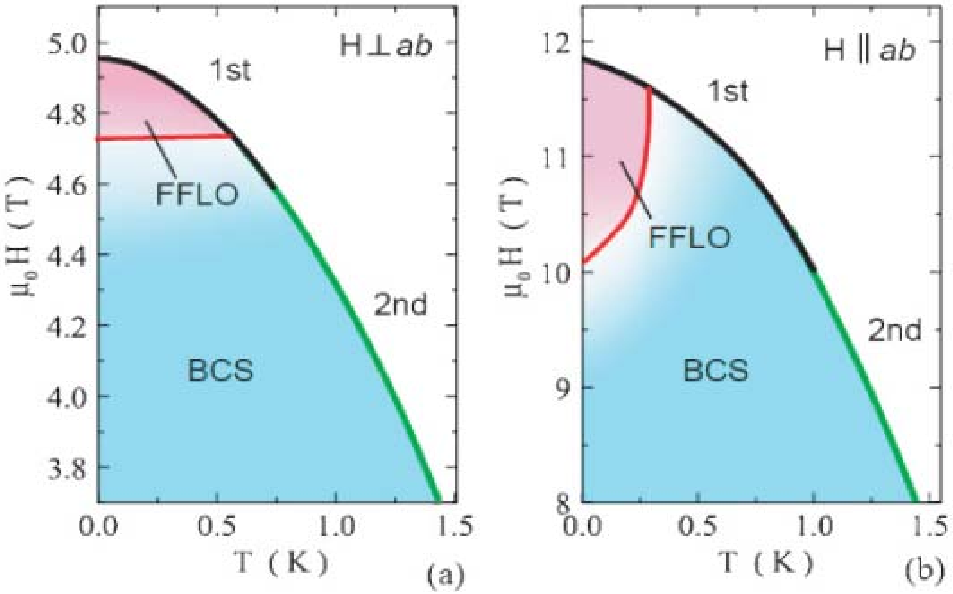

Fig. 9. Experimentally determined H–T phase diagrams of $CeCoIn_5$ at low temperatures and high field for (a) $\boldsymbol{H} \perp ab$ and (b) $\boldsymbol{H} \parallel ab$. The colored portions display the FFLO (pink) and BCS (blue) regions. The black and green lines represent the upper critical fields, which are first order and second order, respectively. The red lines represent the phase boundary separating the FFLO and BCS states.

Phase diagrams of the S/F/N sandwiches

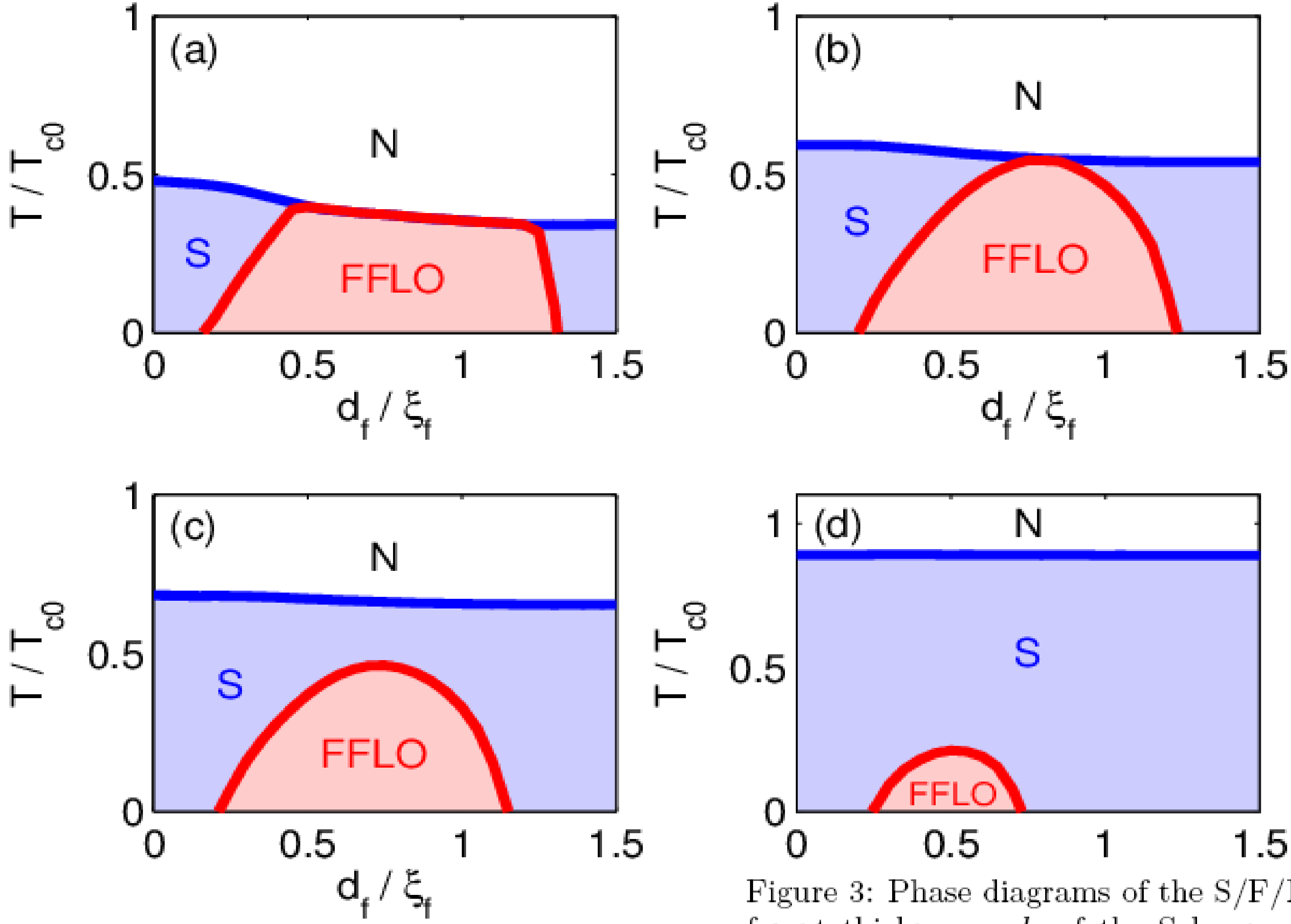

Figure 3: Phase diagrams of the S/F/N sandwiches with different thicknesses d_s of the S layer. The ratio $d_s/(\sqrt{2\pi}\xi_s)$ takes the values: (a) 1.2; (b) 1.4; (c) 1.6; (d) 2.8. Other parameters are: $\sigma_f/\sigma_s = 1$, $\sigma_n/\sigma_s = 150$, $h/T_{c0} = 25$, $d_n/(\sqrt{2\pi}\xi_s) = 1$.

Towards the experimental observation of the FFLO phase

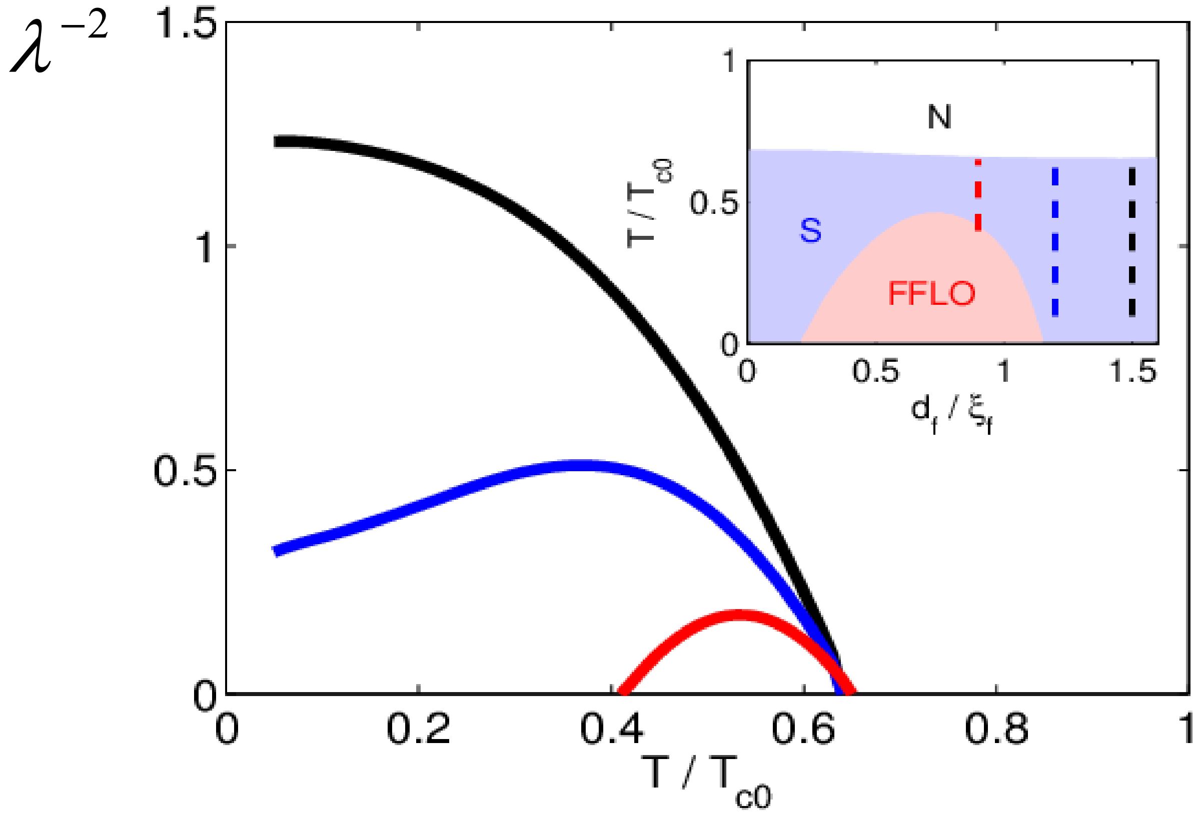

S: NbN, TaN, WSi … [~ 10 nm]

F: CuNi, PdFe … [~ 5 nm]

N: Ag, Au, Al … [~ 20 nm]

Dependence of supercurrent on supervelocity

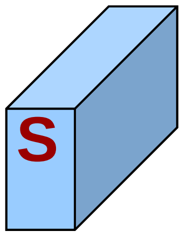

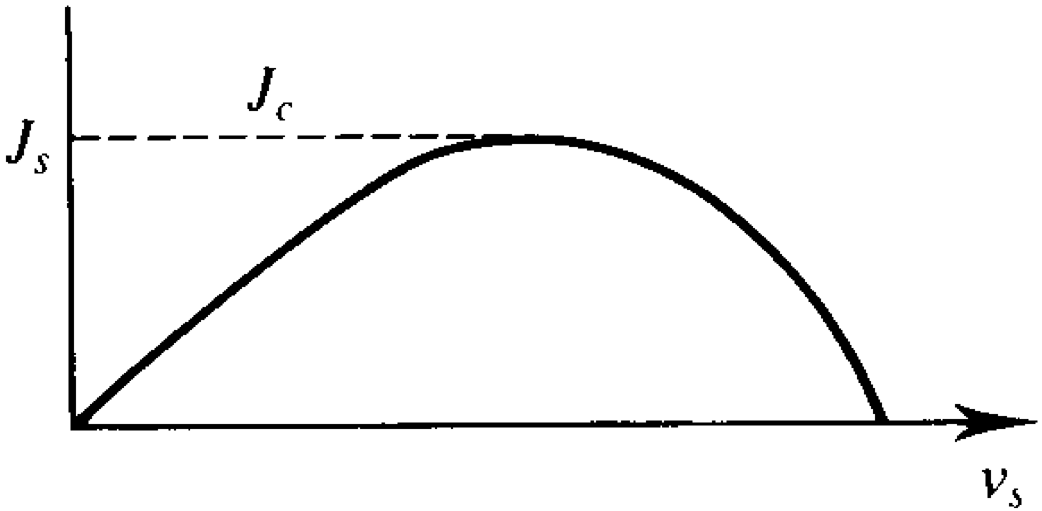

$$J_s = 2e\psi_\infty^2\left(1-\frac{m^* v_s^2}{2|\alpha|}\right)v_s$$

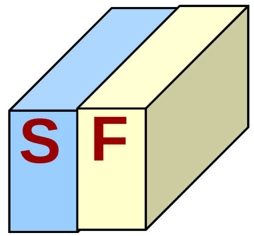

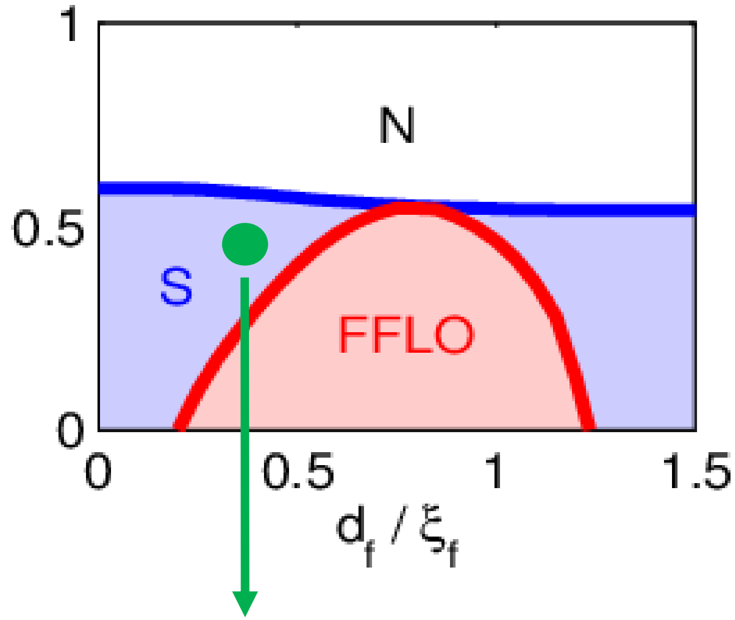

$$J\left(v_s\right) = ?$$

Dependence of supercurrent on supervelocity

$$J \sim \lambda^{-2}\left(v_s\right)v_s$$

$$\lambda^{-2} = a\left(v_s\right)\Delta^2\left(v_s\right) + b\left(v_s\right)\Delta^4\left(v_s\right)$$

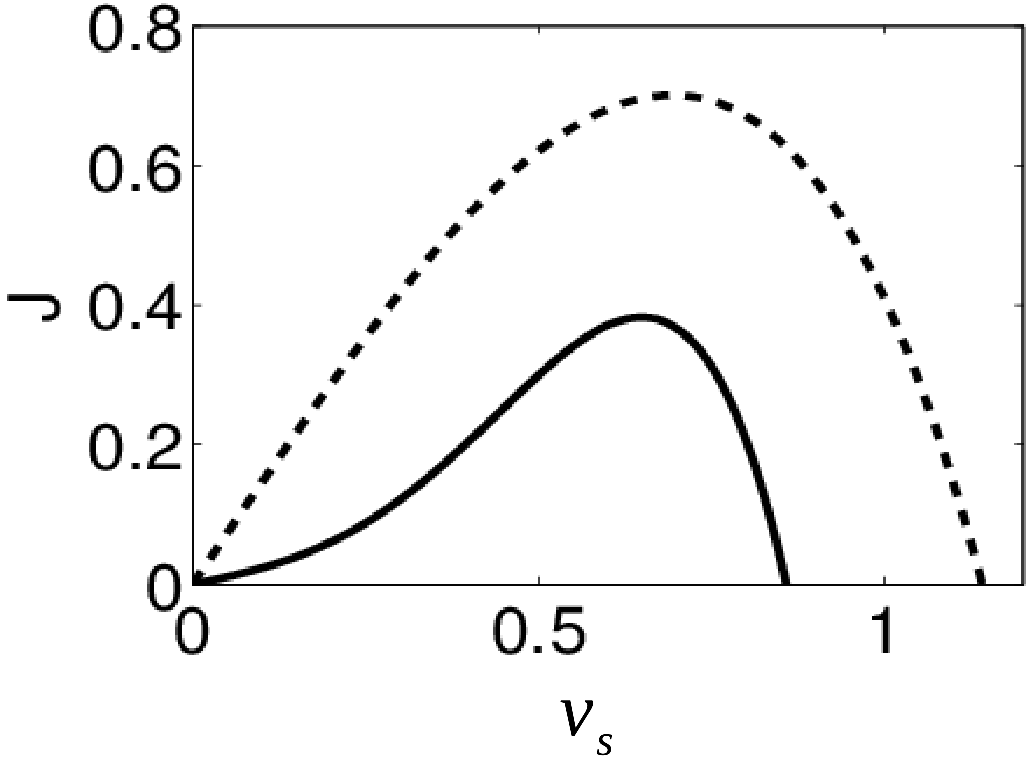

Change of the sign of the third harmonic?

Summary

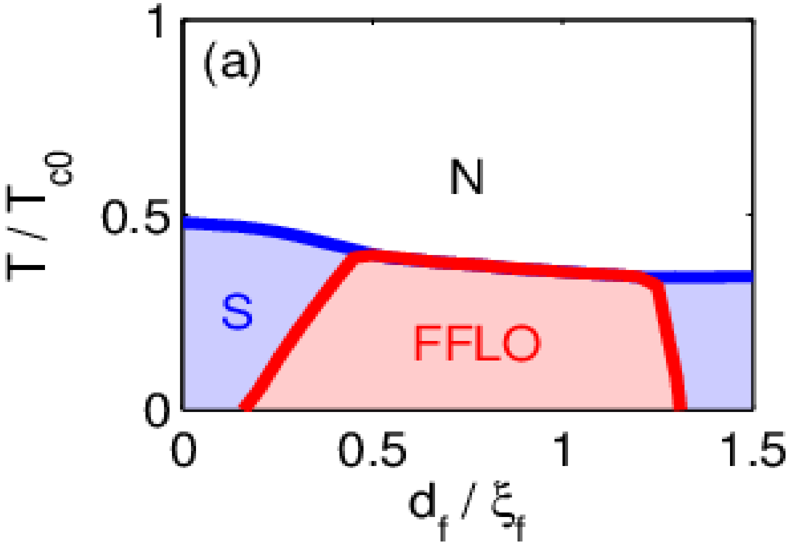

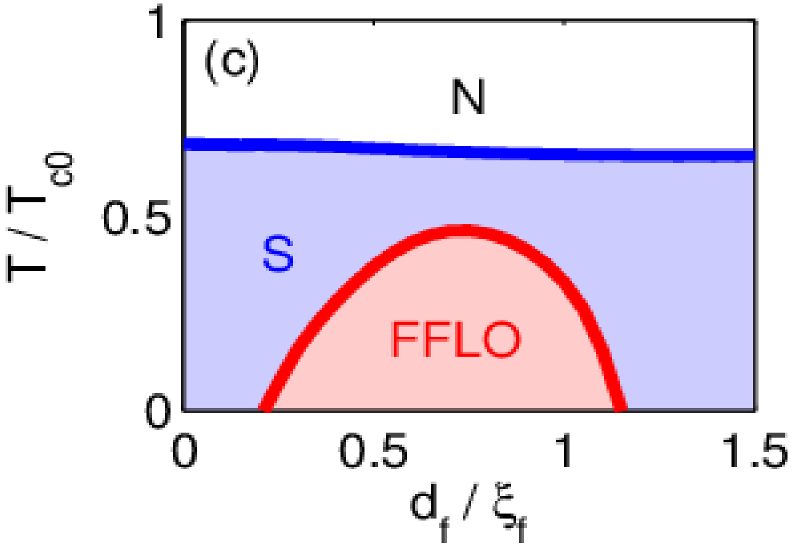

S: NbN, TaN, WSi

F: CuNi, PdFe

N: Ag, Au, Al

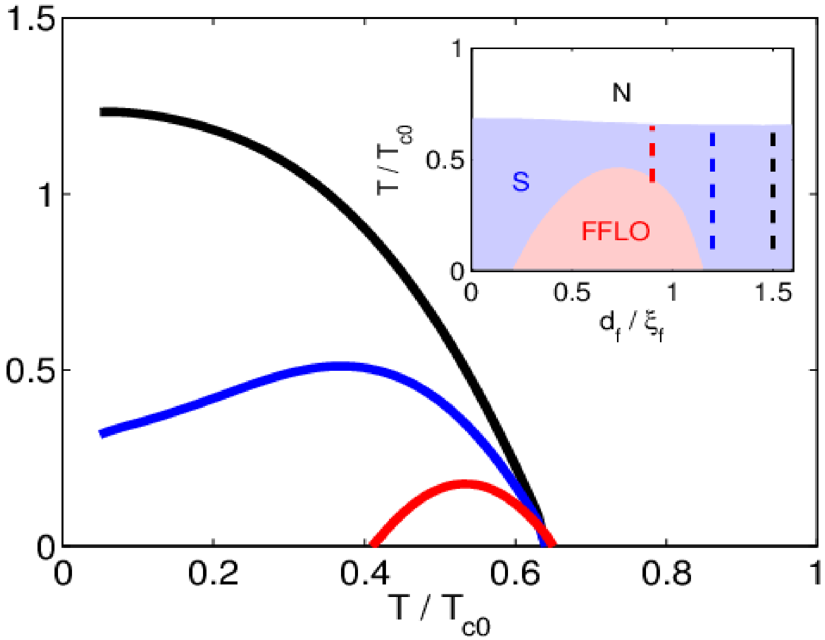

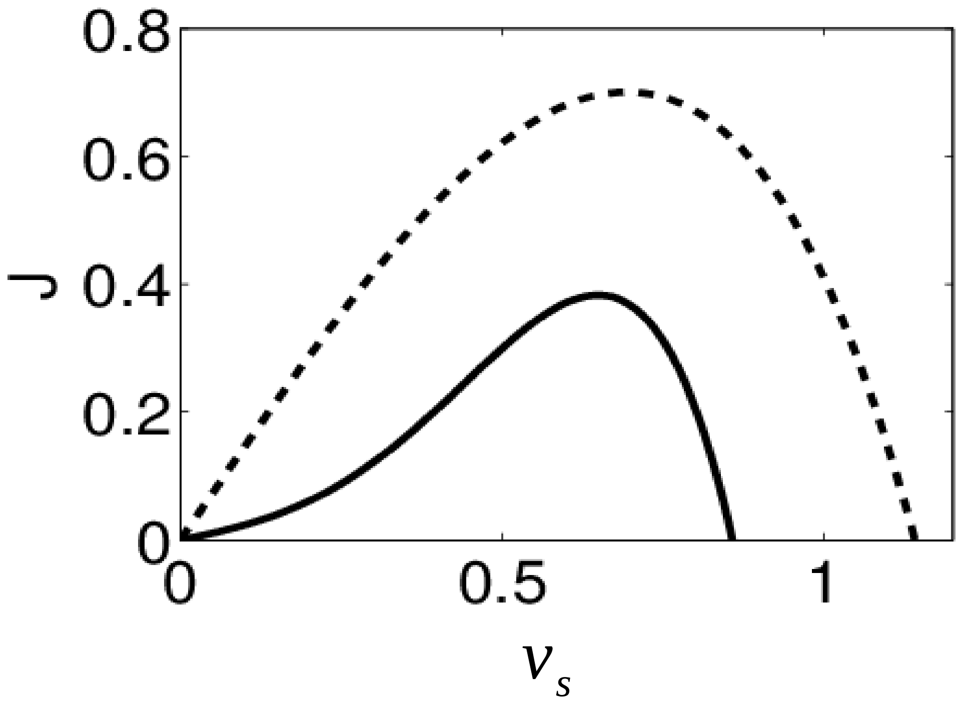

Key points

- **domain superconductivity**
- **LOFF instability**
- **spontaneous currents**